Strain Localization at the crack tip in single crystals : Classical/generalized crystal plasticity solutions vs. experimental results for nickel–base superalloys

Sylvain Flouriot, Samuel Forest,
Georges Cailletaud, Luc Rémy

samuel.forest@ensmp.fr
Centre des matériaux/UMR 7633
Ecole des Mines de Paris/CNRS
http ://www.mat.ensmp.fr

Contents

1. Single crystal nickel–base superalloys
2. Rice's solution for the crack tip stress field
3. Cosserat crystal plasticity : application to crack tip fields
4. Difficulties arising when comparing predictions with experimental results
5. Computations and experiments on CT specimens
6. Consequences for fatigue crack propagation

Single Crystal Superalloys

Chemical composition of AM1

		Ni	Co	Cr	Mo	W	Ta	Al	Ti	C	Fe
mass fraction %	min	balance	6.	7.	1.8	5.	7.5	5.1	1.0		
	max		7.	8.	2.2	6.	8.5	5.5	1.4	0.01	0.2

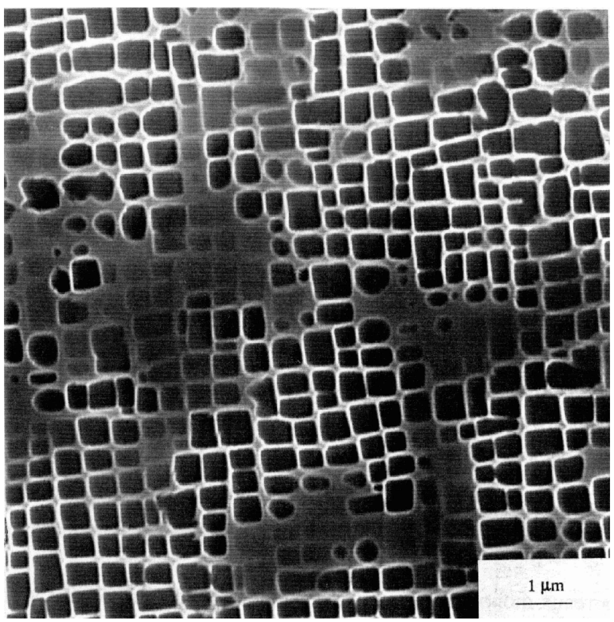

Typical morphology of AM1

Two phases :

– the γ matrix is a F.C.C. disordered phase

– coherent γ' precipitates ($\sim 70\%$)

Slip systems in Nickel–base superalloys

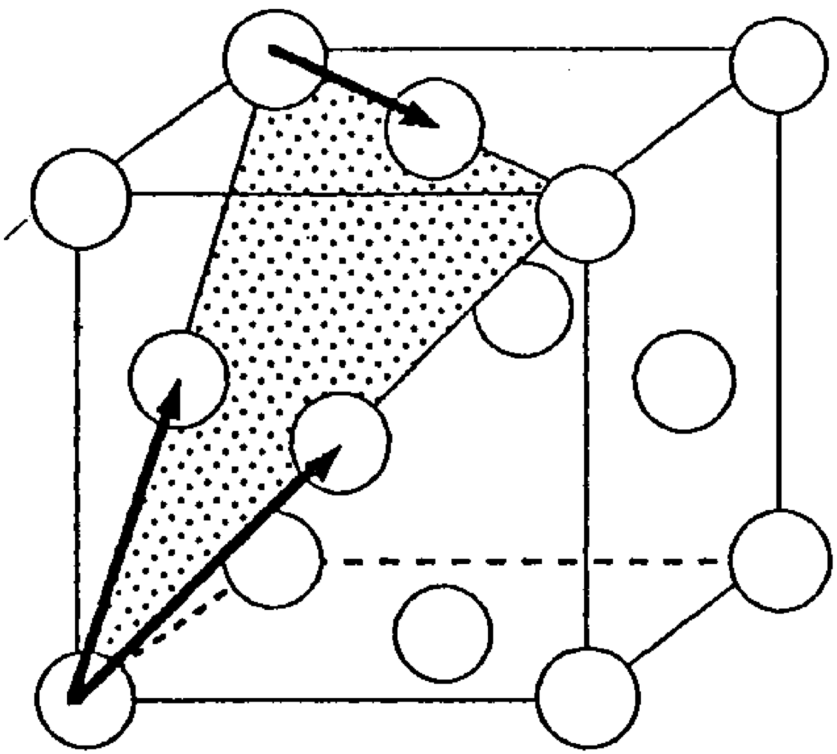

12 octahedral slip systems
– slip planes $\{111\}$
– slip directions $< 110 >$
6 cube slip systems
– slip planes $\{001\}$
– slip directions $< 110 >$

Schmid law :$\tau^s = \underset{\sim}{\boldsymbol{\sigma}} : \underset{\sim}{\boldsymbol{m}}^s = \tau_c$ resolved shear stress on the system s

$$\underset{\sim}{\boldsymbol{m}}^s = \frac{1}{2}(\underline{\boldsymbol{m}}^s \otimes \underline{\boldsymbol{n}}^s + \underline{\boldsymbol{n}}^s \otimes \underline{\boldsymbol{m}}^s)$$

$\underline{\boldsymbol{m}}^s$ the slip direction

$\underline{\boldsymbol{n}}^s$ the normal to the slip plane

AM1 behavior

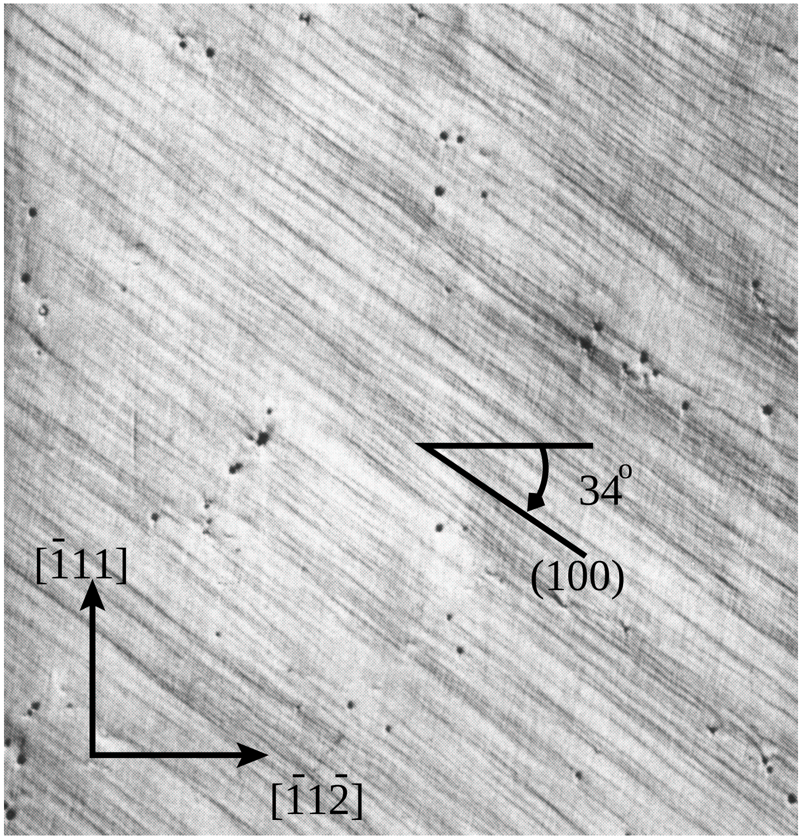

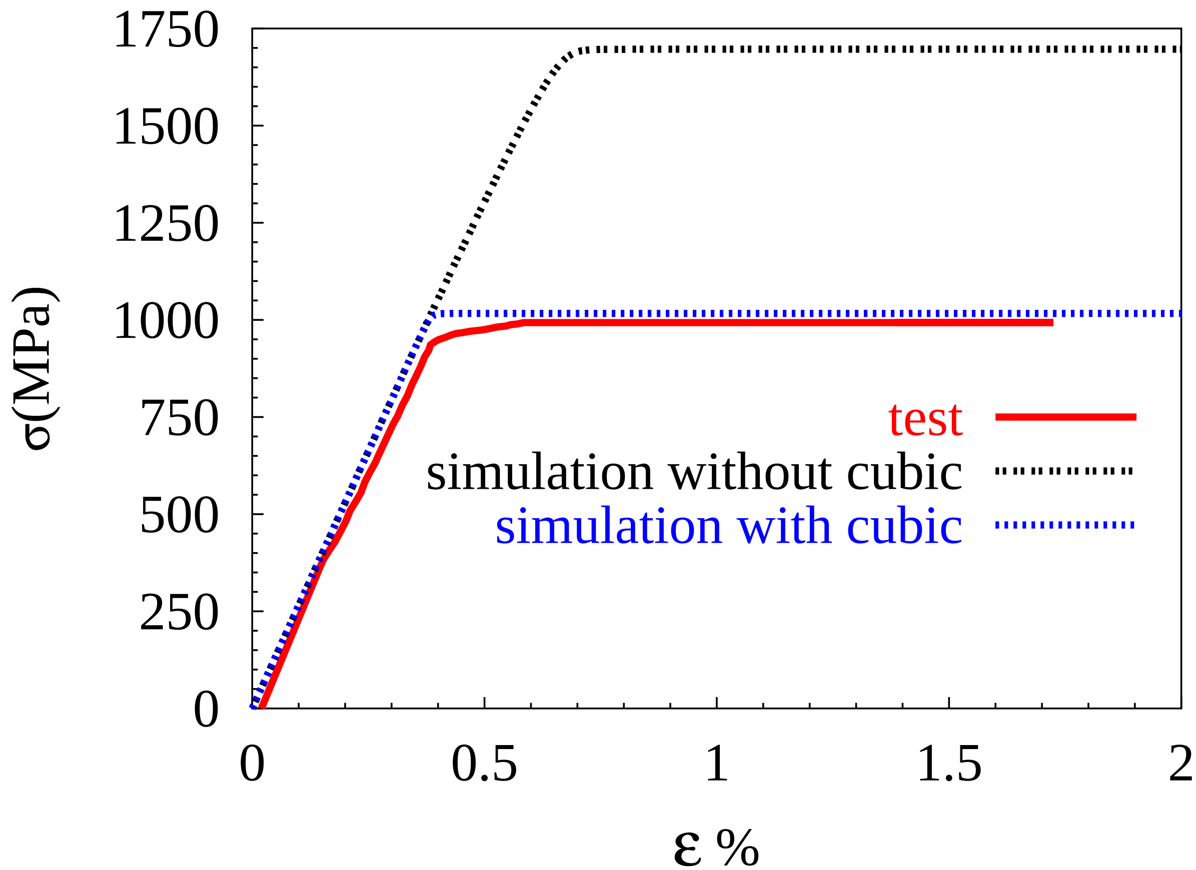

experimental & simulation tension test on AM1 <111> at 650^oC

$\Rightarrow$ *Existence of cube slip systems*

Continuum Crystal Plasticity Framework

[Mandel, 1973] [Asaro, 1983] [Méric & Cailletaud, 1991]

multiplicative decomposition of the deformation gradient

$$\underset{\sim}{\boldsymbol{F}} = \underset{\sim}{\boldsymbol{F}}^e \underset{\sim}{\boldsymbol{F}}^p$$

Viscoplastic strain :

$$\dot{\underset{\sim}{\boldsymbol{F}}}^p \underset{\sim}{\boldsymbol{F}}^{p-1} = \sum_s \dot{\gamma}^s \underline{\boldsymbol{m}}^s \otimes \underline{\boldsymbol{n}}^s$$

Flow rule :

$$\dot{\gamma}^s = \langle \frac{|\tau^s - x^s| - r^s}{K} \rangle^n sign(\tau^s - x^s)$$

Isotropic Hardening :

$$r^s = r_o + Q \sum_{r=1}^{N} h^{sr}(1 - exp(-bv^r))$$

$$\dot{v}^s = |\dot{\gamma}^s|$$

Kinematic Hardening

$$\dot{\alpha}^s = \dot{\gamma}^s - d\dot{v}^s \alpha^s$$

$$x^s = c\alpha^s$$

Rice's solution

[Rice, 1987] [Rice, Hawk & Asaro, 1990]

– *Mode I crack in a single crystal*

– *Plane strain :*

$$\begin{pmatrix} \varepsilon_{11} & \varepsilon_{12} & 0 \\ \varepsilon_{12} & \varepsilon_{22} & 0 \\ 0 & 0 & 0 \end{pmatrix}_{X_1,X_2,X_3} \rightarrow \begin{pmatrix} \sigma_{11} & \sigma_{12} & 0 \\ \sigma_{12} & \sigma_{22} & 0 \\ 0 & 0 & \sigma_{33} \end{pmatrix}_{X_1,X_2,X_3}$$

– *Elastic-ideally plastic crystals*

– *Small strains*

– *Octahedral slip systems - cube slip systems*

– *Schmid Rule*

$(001)_{X_2}[110]_{X_1} \& [110]_{X_2}(001)_{X_1}$ *crack orientations*

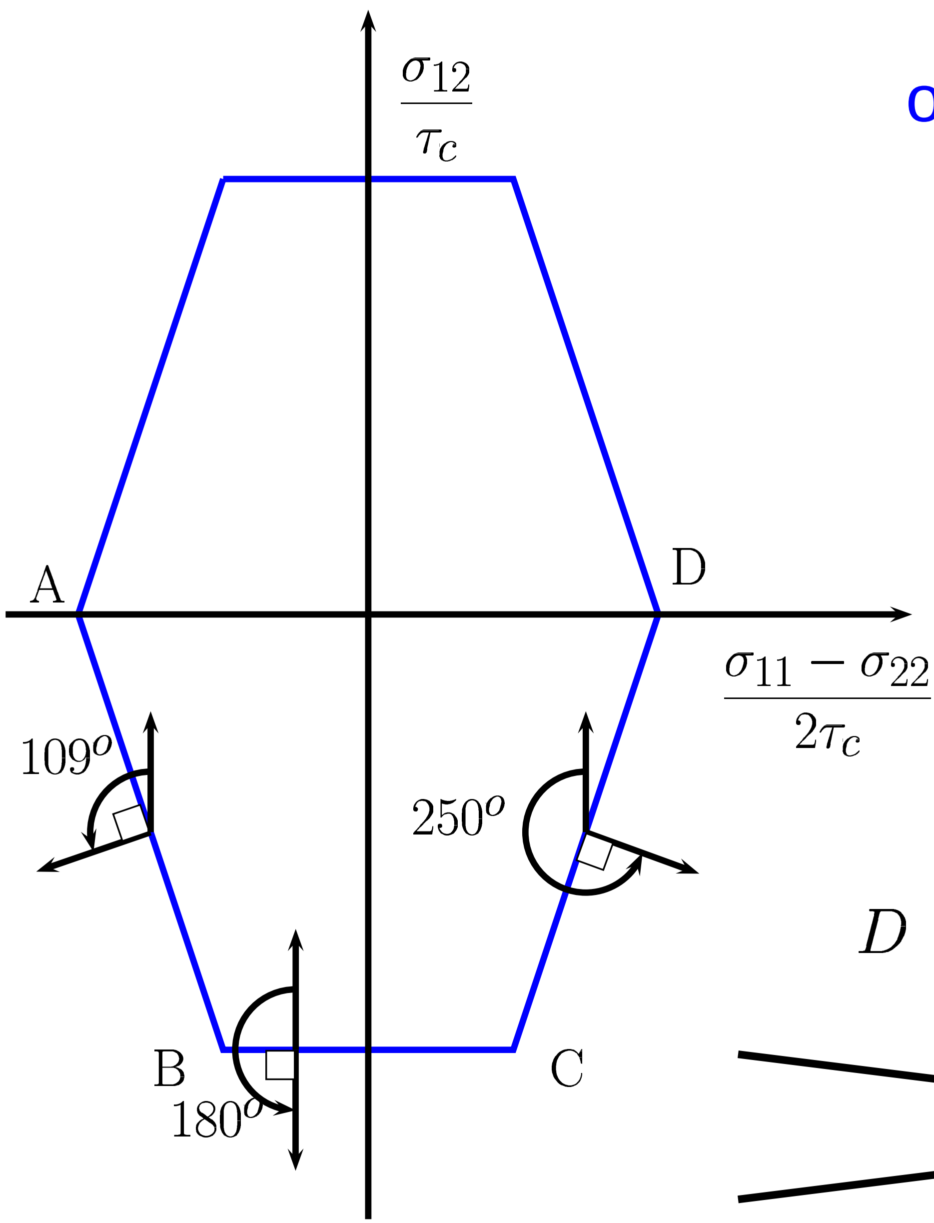

octahedral slip systems

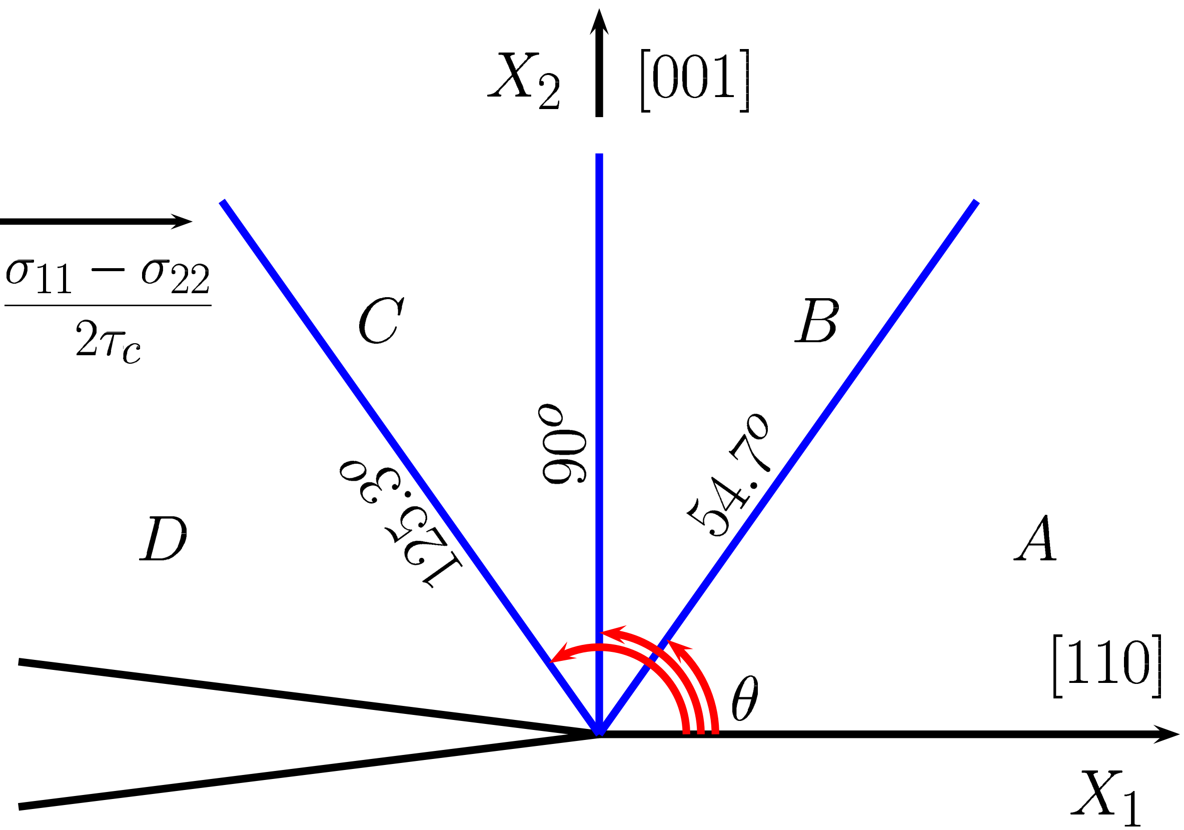

$(001)_{X_2}[110]_{X_1}$ & $(110)_{X_2}[001]_{X_1}$ *crack orientation*

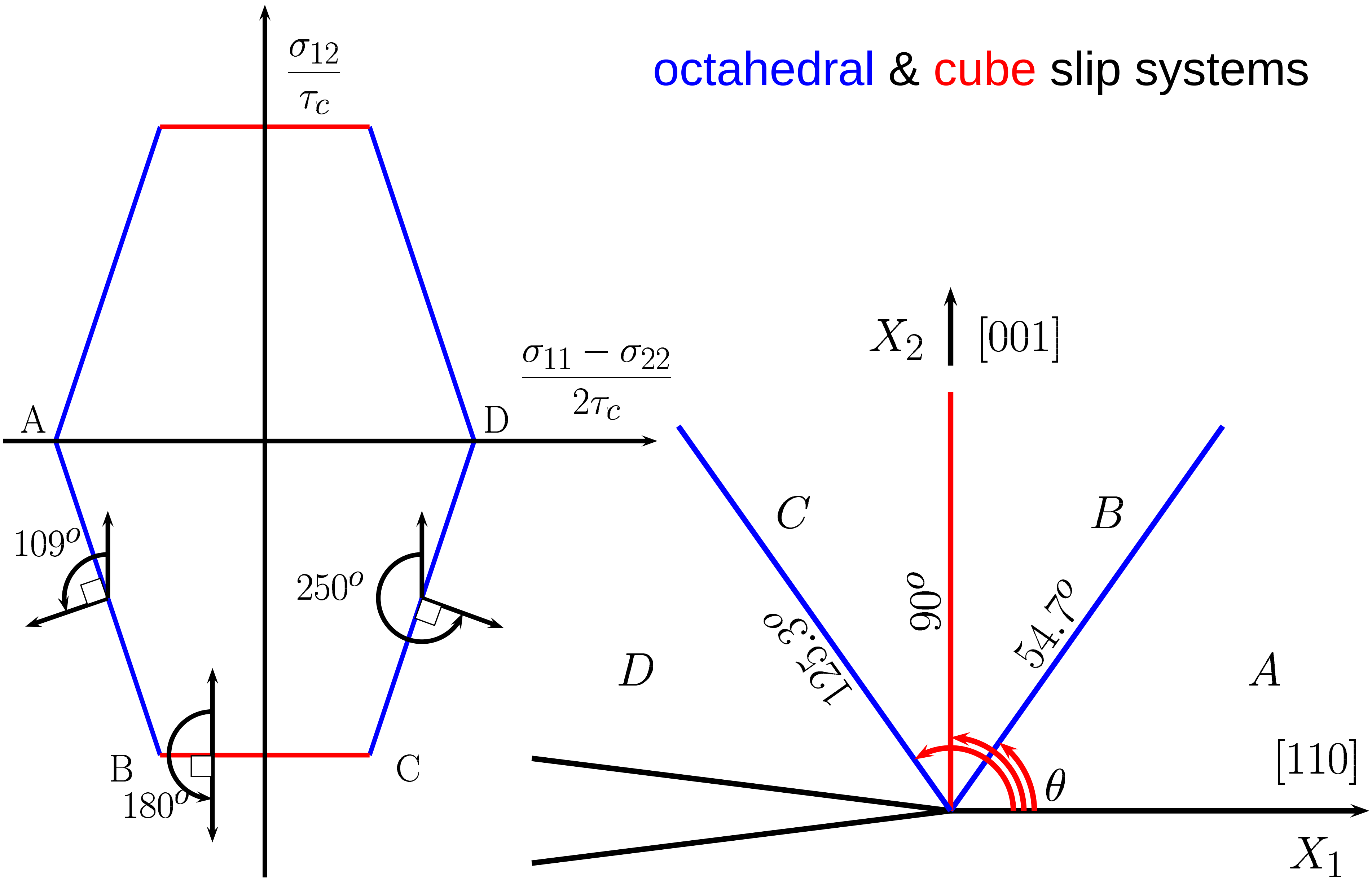

$(001)_{X_2}[100]_{X_1}$ *crack orientation*

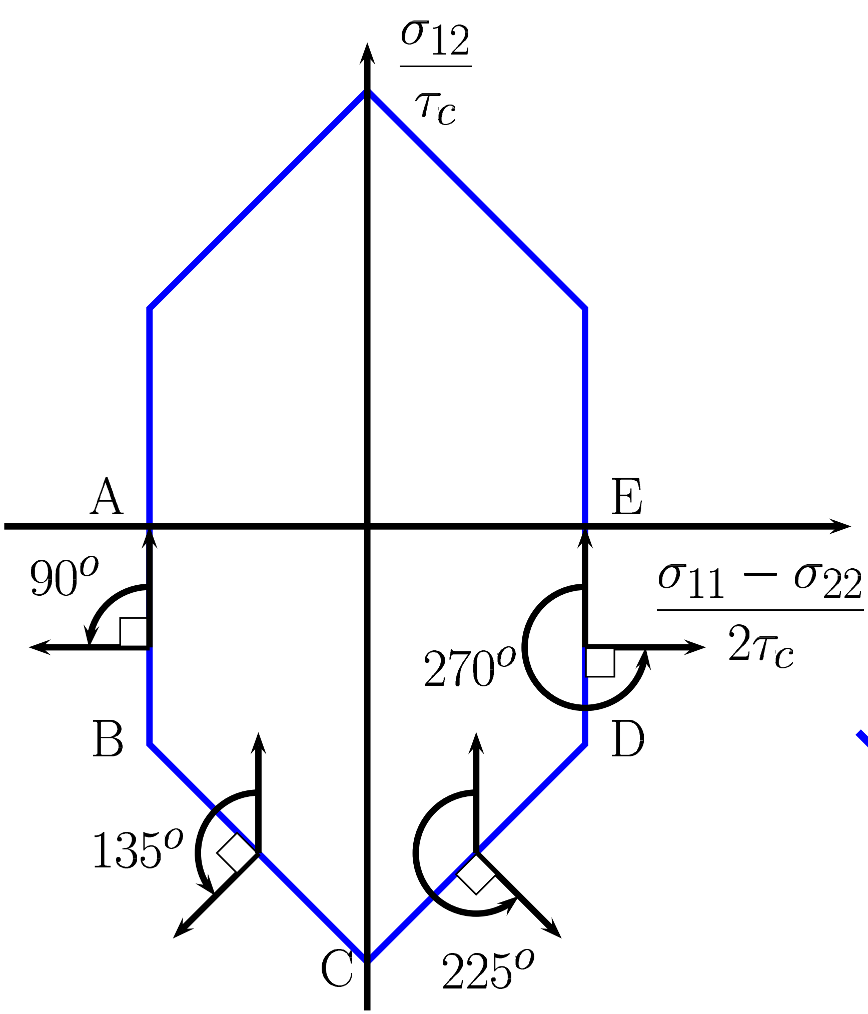

octahedral slip systems

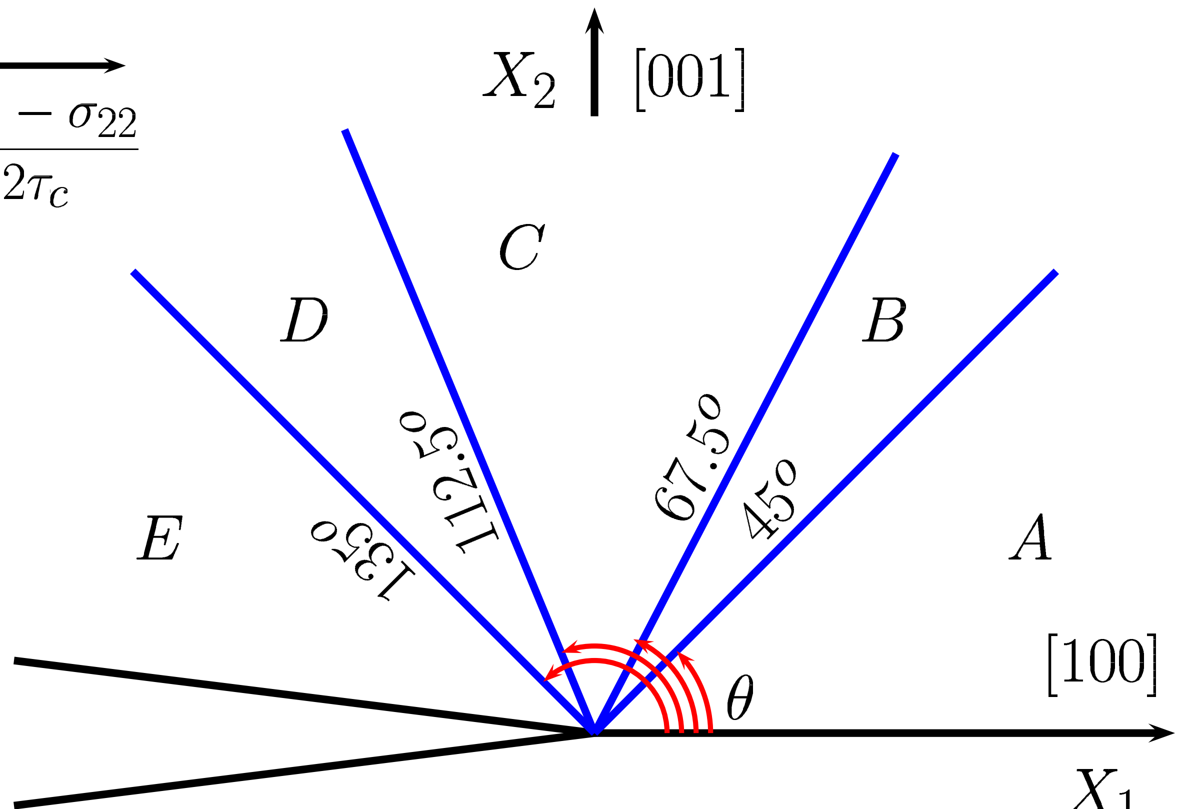

$(001)_{X_2}[100]_{X_1}$ *crack orientation*

octahedral & cube slip systems at 650^oC

$$\frac{\tau_{cube}}{\tau_{oc}} = .83 \leq \frac{\sqrt{3}}{2}$$

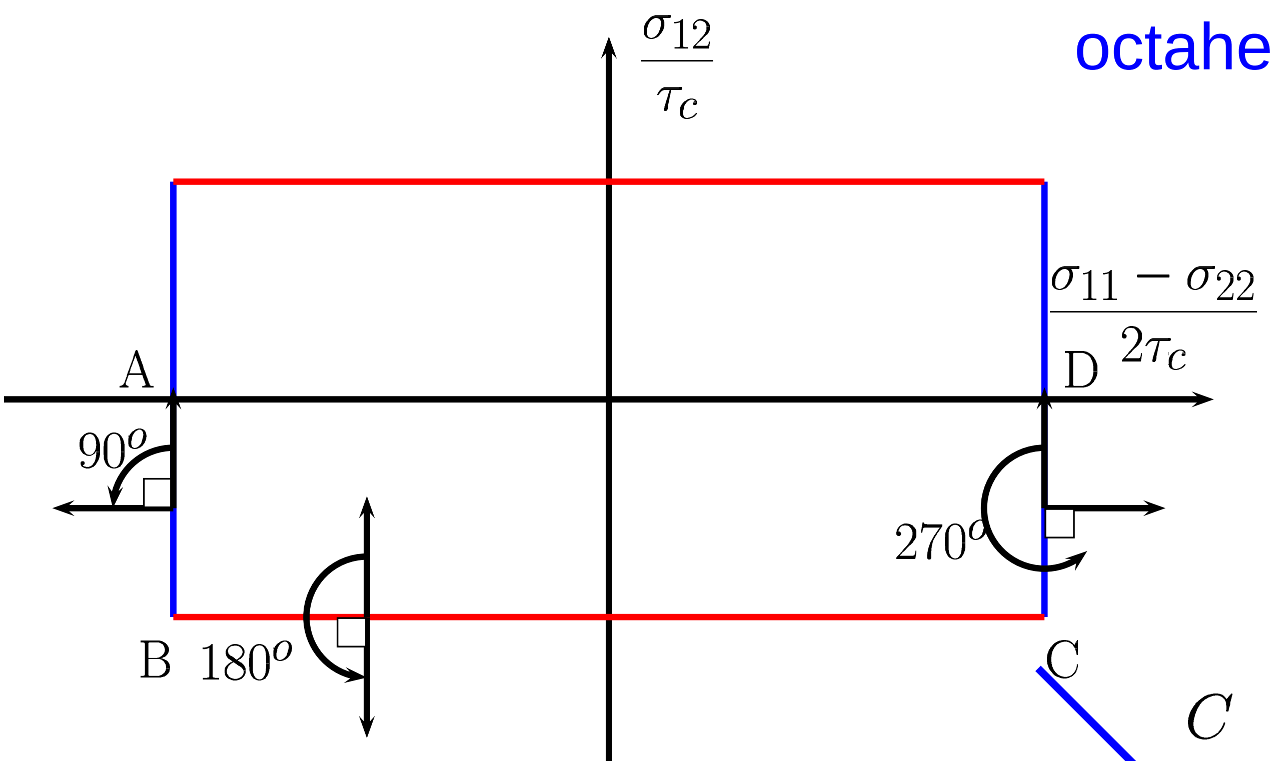

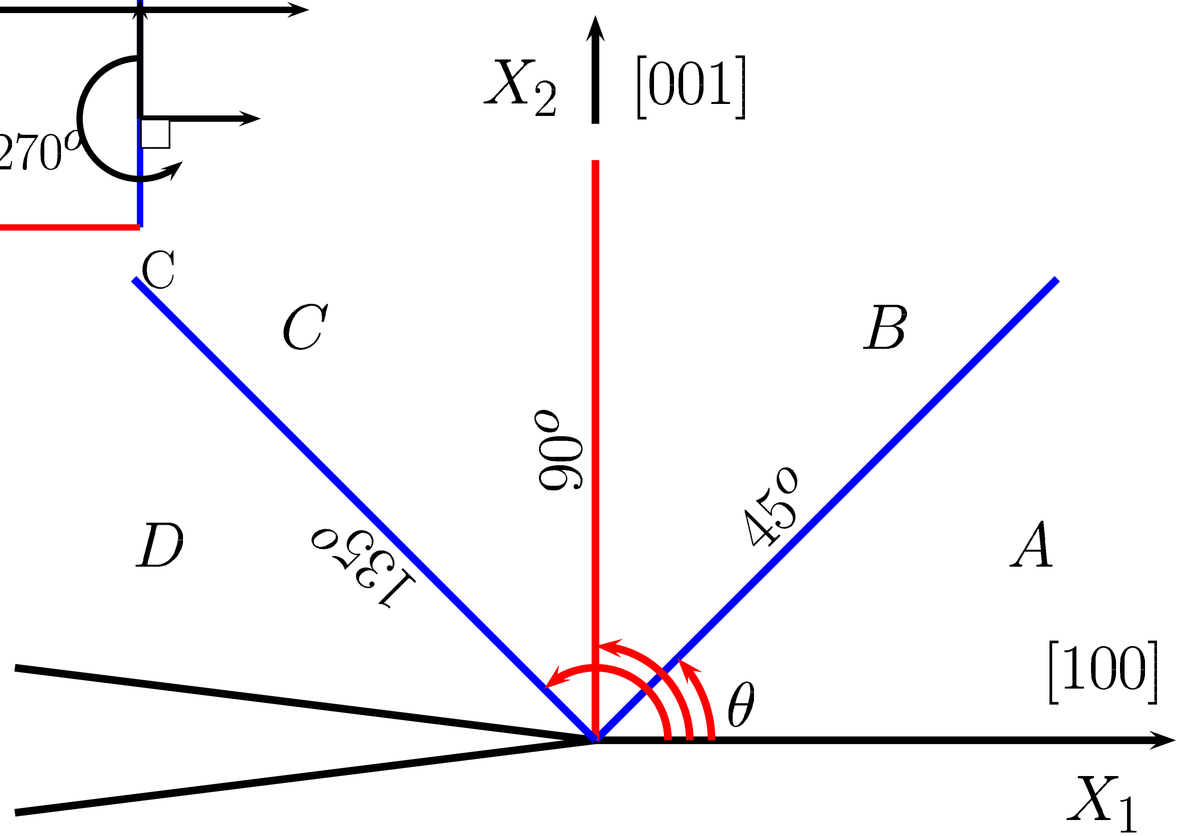

$(001)_{X_2}[100]_{X_1}$ *crack orientation*

octahedral & cube slip systems
at 20^oC

$$\frac{\sqrt{3}}{2} \leq \frac{\tau_{cube}}{\tau_{oc}} = 1.53 \leq \sqrt{3}$$

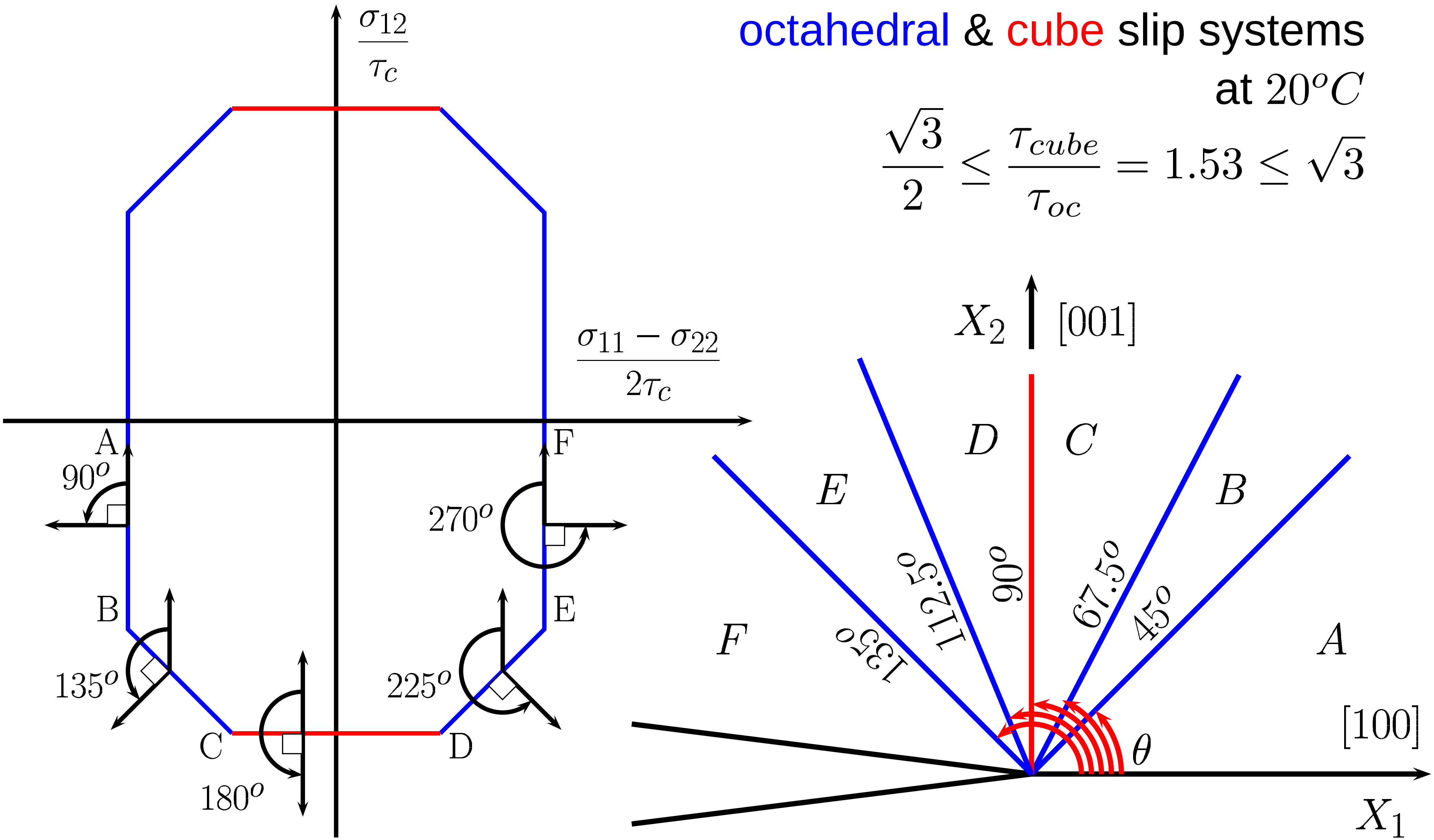

Finite Element Simulations ($(001)_{X_2}[110]_{X_1}$ crack orientation)

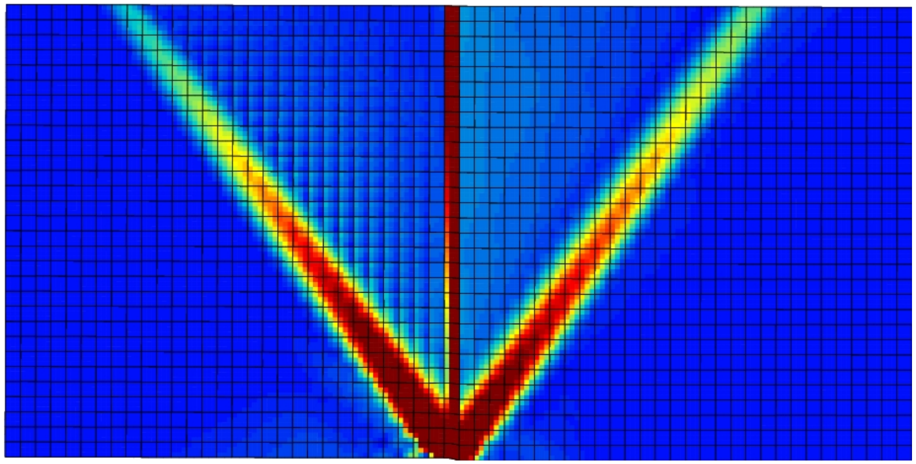

cumulative octahedral slip $\sum_{s=1}^{12} |\gamma^s|$

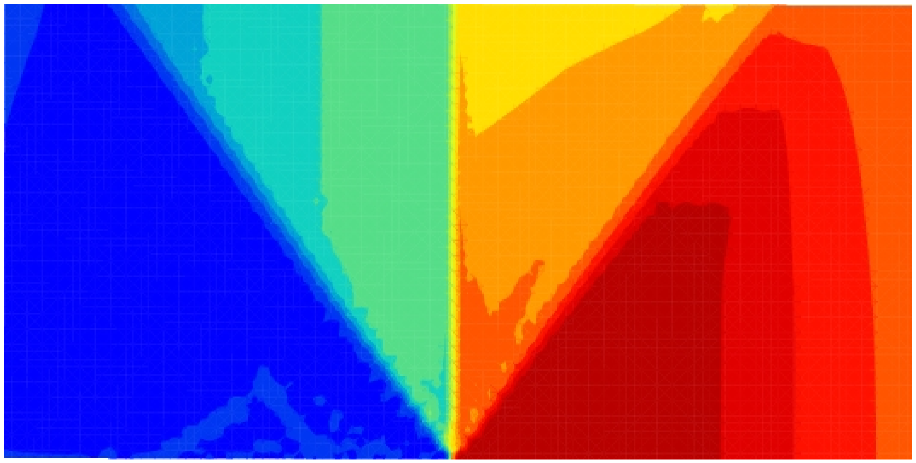

stress σ_{22}

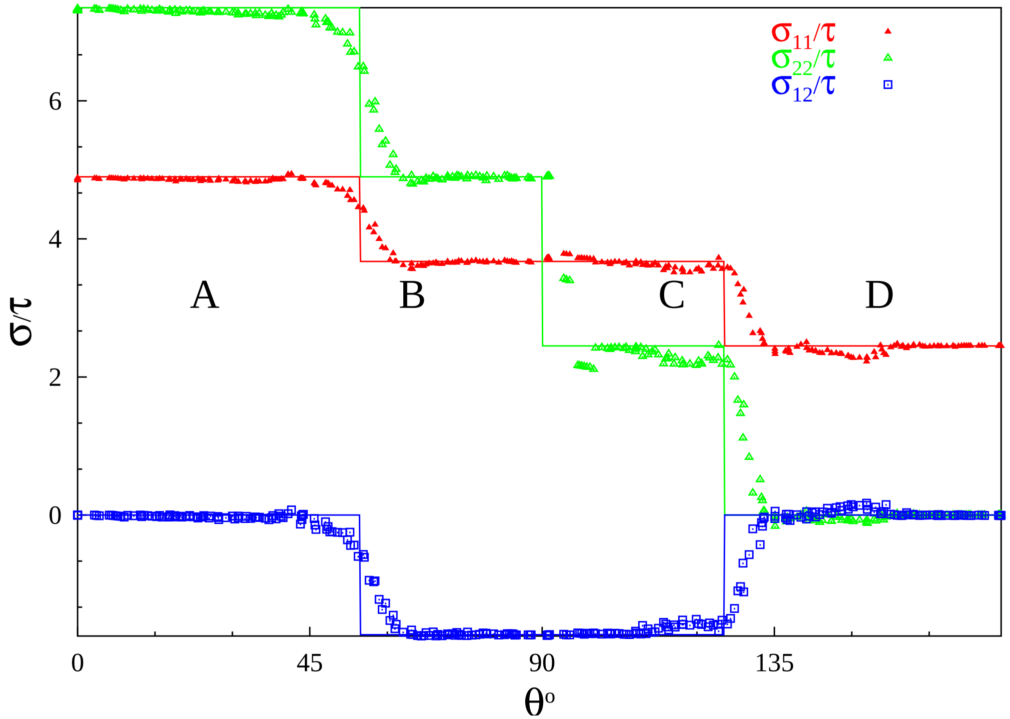

Finite Element simulations ($(001)_{X_2}[100]_{X_1}$ crack orientation)

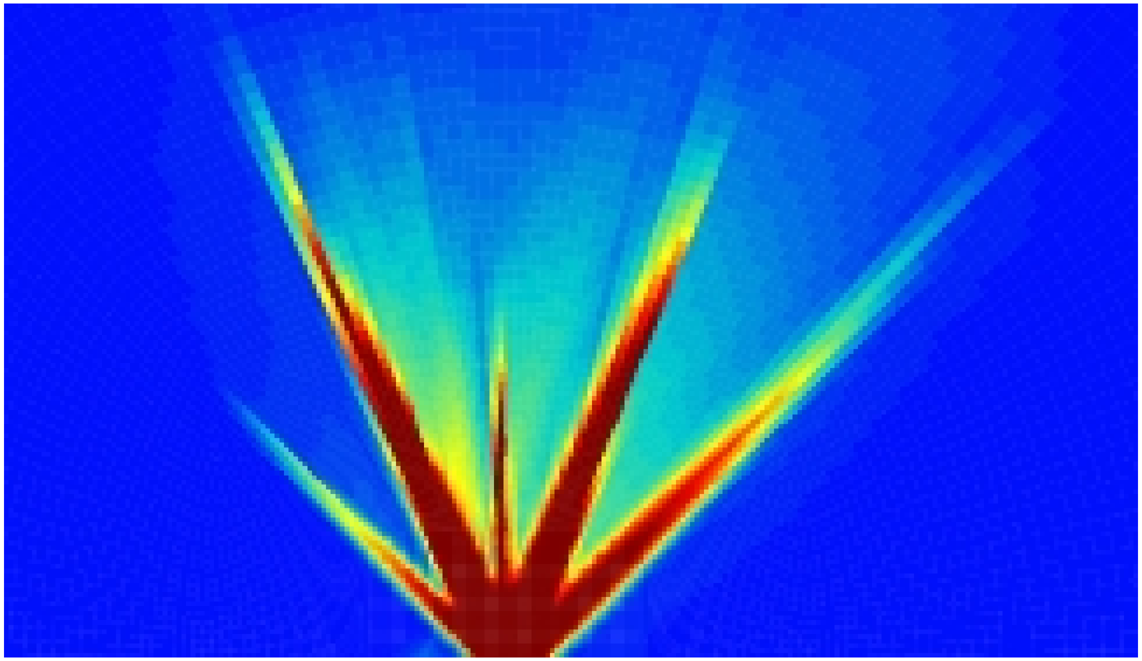

ε_{in}^{eq}

octahedral & cube slip systems at $20^o C$

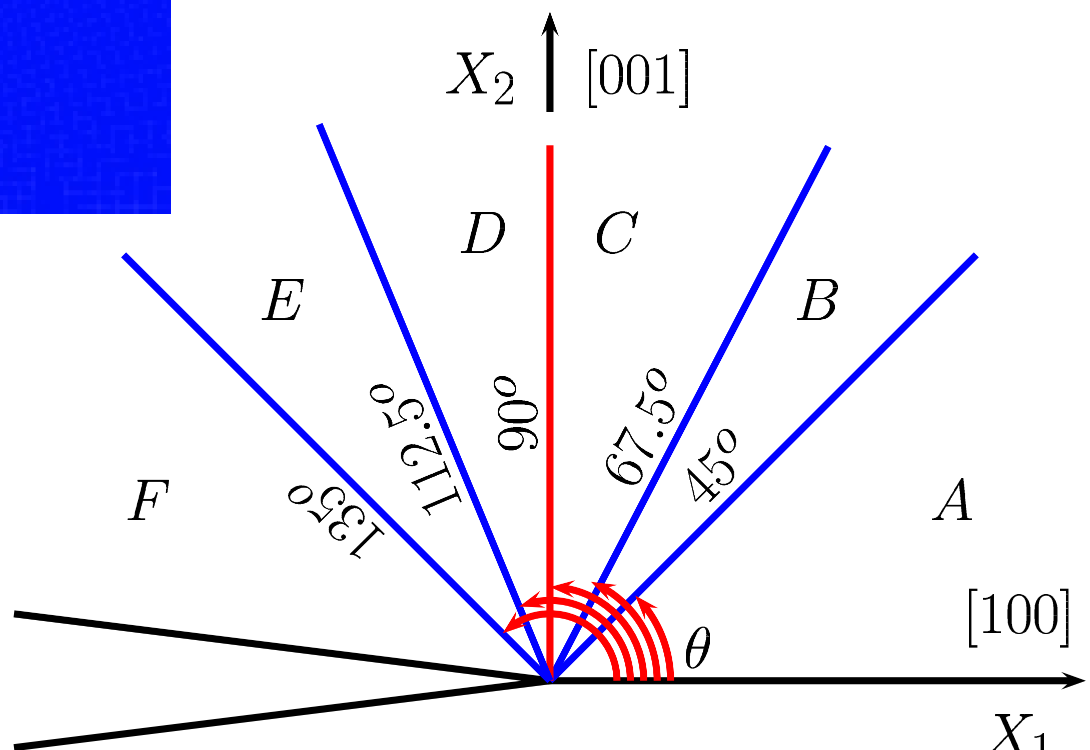

$(001)_{X_2}[110]_{X_1}$ & $(110)_{X_2}[001]_{X_1}$ *crack orientations*

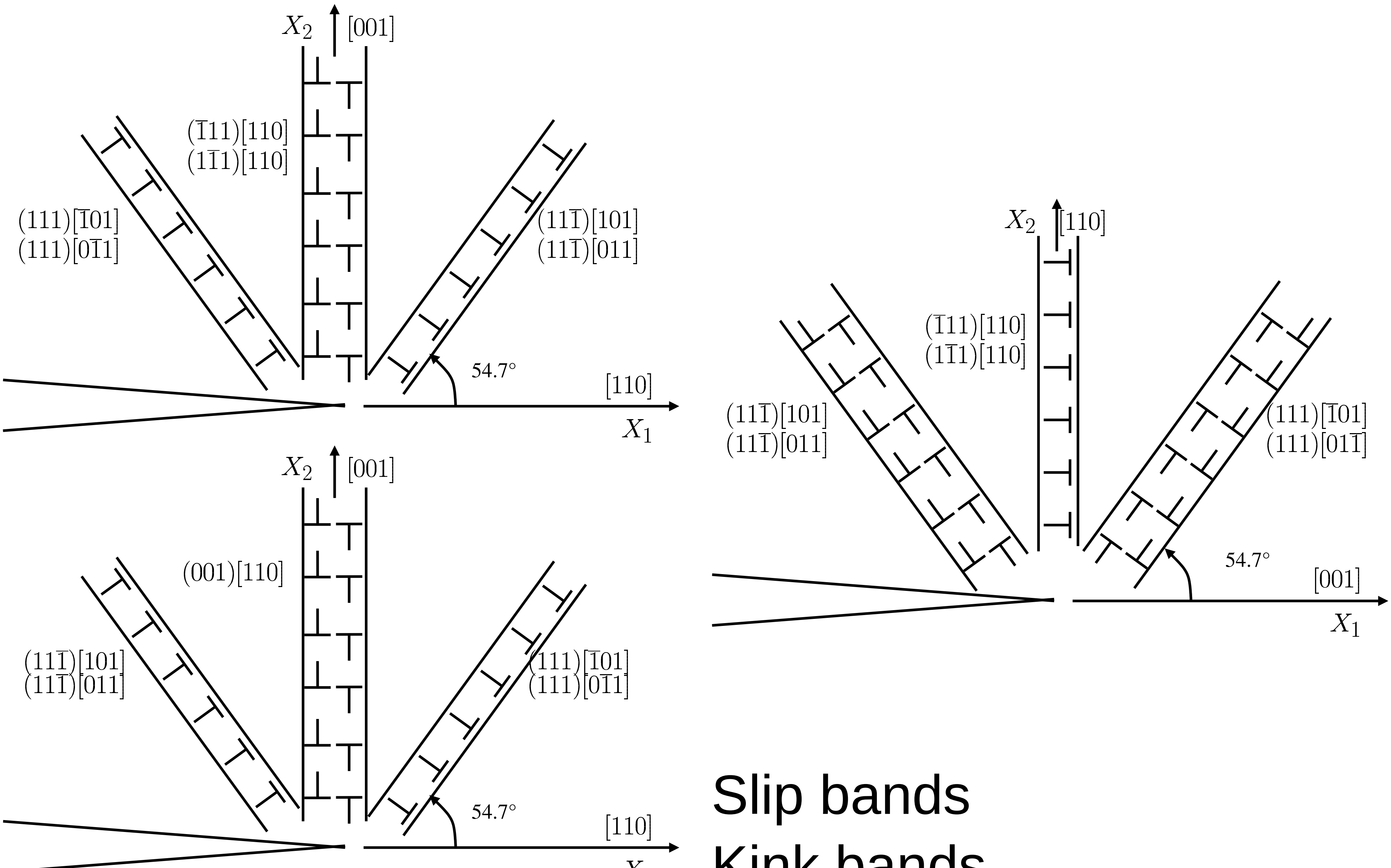

Slip bands

Kink bands

Non local models at the crack tip in single crystals

Introduction of the influence of Nye's dislocation density tensor on material hardening into continuum crystal plasticity modelling

[Nye, 1953] [Kröner, 1958], GNDs [Ashby, 1970]

1. Gradient of internal variable approach [Aifantis, 1987] [Steinmann, 2000] [Gurtin, 2000]
2. Higher grade media [Xia, Hutchinson, 1996] [Fleck, Hutchinson, 1997]
3. Higher order media [Kröner, 1963] [Mura, 1966] [Eringen, 1970] [Forest, 1996]

Cosserat continuum

kinematics

d.o.f. $\underline{\boldsymbol{u}}, \underline{\boldsymbol{\Phi}}$

Cosserat deformation :

$$e_{ij} = u_{i,j} + \epsilon_{ijk}\Phi_k$$

curvature tensor :

$$\kappa_{ij} = \Phi_{i,j}$$

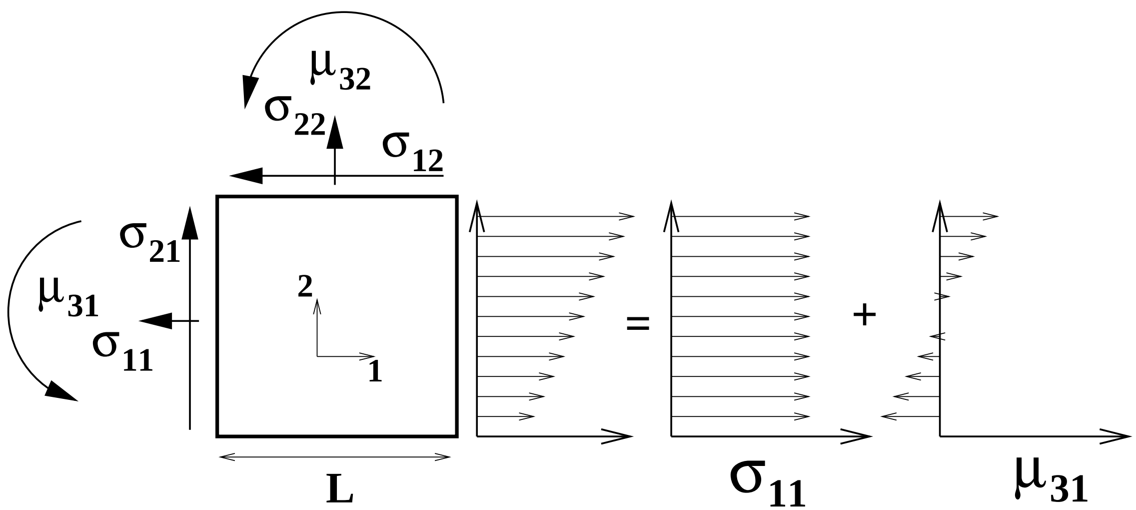

isotropic elasticity :

$$\underset{\sim}{\boldsymbol{\sigma}} = \lambda \, \underset{\sim}{\mathbf{1}} \, \mathrm{Tr} \, \underset{\sim}{\boldsymbol{e}}^e + 2\mu \, {}^{\{}\underset{\sim}{\boldsymbol{e}}^{e\}} + 2\mu_c \, {}^{\}}\underset{\sim}{\boldsymbol{e}}^{e\{}$$

$$\underset{\sim}{\boldsymbol{\mu}} = \alpha \, \underset{\sim}{\mathbf{1}} \, \mathrm{Tr} \, \underset{\sim}{\boldsymbol{\kappa}}^e + 2\beta \, {}^{\{}\underset{\sim}{\boldsymbol{\kappa}}^{e\}} + 2\gamma \, {}^{\}}\underset{\sim}{\boldsymbol{\kappa}}^{e\{}$$

statics

balance of momentum :

$$\sigma_{ij,j} + f_i = 0$$

balance of moment of momentum :

$$\mu_{ij,j} - \epsilon_{ijk}\sigma_{jk} + c_i = 0$$

Cosserat crystal plasticity

$$ {}^\sharp\underset{\sim}{\boldsymbol{F}} = \underset{\sim}{\boldsymbol{R}}^T\, \underset{\sim}{\boldsymbol{F}}, \quad {}^\sharp\underset{\sim}{\boldsymbol{\Gamma}} = \underset{\sim}{\boldsymbol{R}}^T\, \underset{\sim}{\boldsymbol{\Gamma}} $$

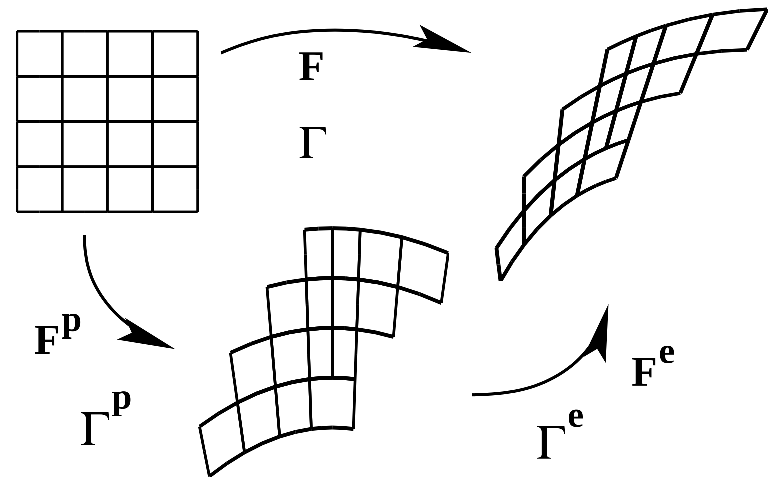

multiplicative/additive decomposition

$$ {}^\sharp\underset{\sim}{\boldsymbol{F}} = {}^\sharp\underset{\sim}{\boldsymbol{F}}^e\, {}^\sharp\underset{\sim}{\boldsymbol{F}}^p, \qquad {}^\sharp\underset{\sim}{\boldsymbol{\Gamma}} = {}^\sharp\underset{\sim}{\boldsymbol{\Gamma}}^e\, {}^\sharp\underset{\sim}{\boldsymbol{F}}^p + {}^\sharp\underset{\sim}{\boldsymbol{\Gamma}}^p $$

generalized Schmid law

$$ {}^\sharp\dot{\underset{\sim}{\boldsymbol{F}}}^p\, {}^\sharp\underset{\sim}{\boldsymbol{F}}^{p-1} = \sum_{s=1}^{n} \dot{\gamma}^s\, {}^\sharp\underset{\sim}{\boldsymbol{P}}^s $$

$$ \tau^s = \underset{\sim}{\boldsymbol{P}}^s : \underset{\sim}{\boldsymbol{\sigma}}^s $$

$$ {}^\sharp\dot{\underset{\sim}{\boldsymbol{\Gamma}}}^p\, {}^\sharp\underset{\sim}{\boldsymbol{F}}^{p-1} = \sum_{s=1}^{n} \left(\frac{\dot{\theta}^s_\perp}{l_\perp} {}^\sharp\underset{\sim}{\boldsymbol{Q}}^s{}_\perp + \frac{\dot{\theta}^s_\odot}{l_\odot} {}^\sharp\underset{\sim}{\boldsymbol{Q}}^s{}_\odot \right) $$

$$ \nu^s = \underset{\sim}{\boldsymbol{Q}}^s : \underset{\sim}{\boldsymbol{\mu}}^s $$

$$ {}^\sharp\underset{\sim}{\boldsymbol{P}}^s = {}^\sharp\underline{\boldsymbol{m}}^s \otimes {}^\sharp\underline{\boldsymbol{n}}^s $$

$$ \dot{\gamma}^s = < \frac{\mid \tau^s \mid - r^s}{k} >^n \ \mathrm{sign}\, \tau^s $$

$$ {}^\sharp\underset{\sim}{\boldsymbol{Q}}_\perp = {}^\sharp\underline{\boldsymbol{\xi}} \otimes {}^\sharp\underline{\boldsymbol{m}}, \quad {}^\sharp\underset{\sim}{\boldsymbol{Q}}_\odot = \frac{1}{2}\underset{\sim}{\boldsymbol{1}} - {}^\sharp\underline{\boldsymbol{m}} \otimes {}^\sharp\underline{\boldsymbol{m}} $$

$$ \dot{\theta}^s = < \frac{\mid \nu^s \mid - l_\perp\, r_c^s}{l_\perp\, k_c^s} >^{n_c^s} \ \mathrm{sign}\, (\nu^s) $$

hardening law

$$ r^s = r_0 + q_1 \sum_{r=1}^{n} h^{sr}(1 - \exp(-b_1 v^r)) + H' \mid \theta^s \mid, \qquad r_c^s = r_{c0} $$

Cosserat crystal plasticity at the crack tip

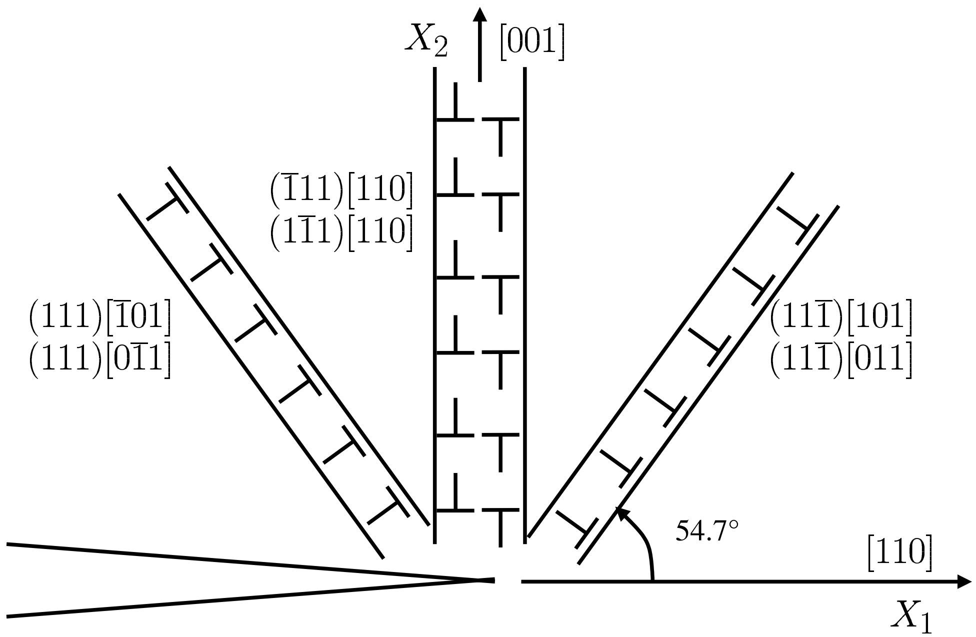

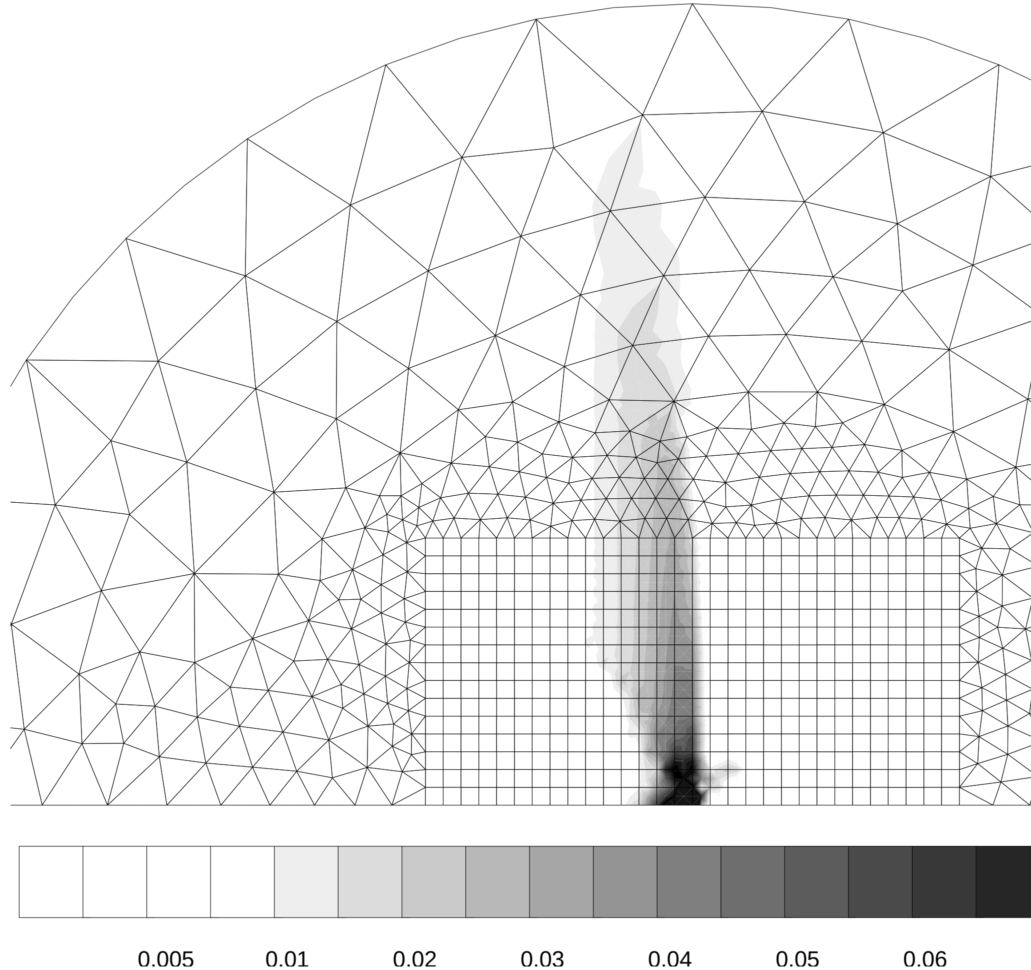

$(001)_{X_2}[110]_{X_1}$ crack orientation

lattice rotation (classical)

Cosserat crystal plasticity at the crack tip

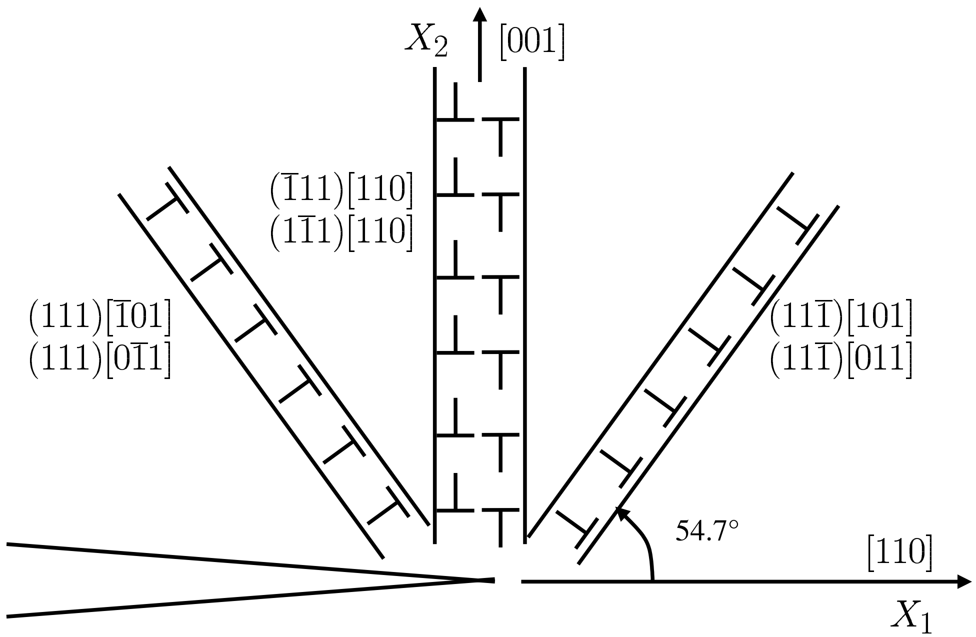

$(001)_{X_2}[110]_{X_1}$ crack orientation

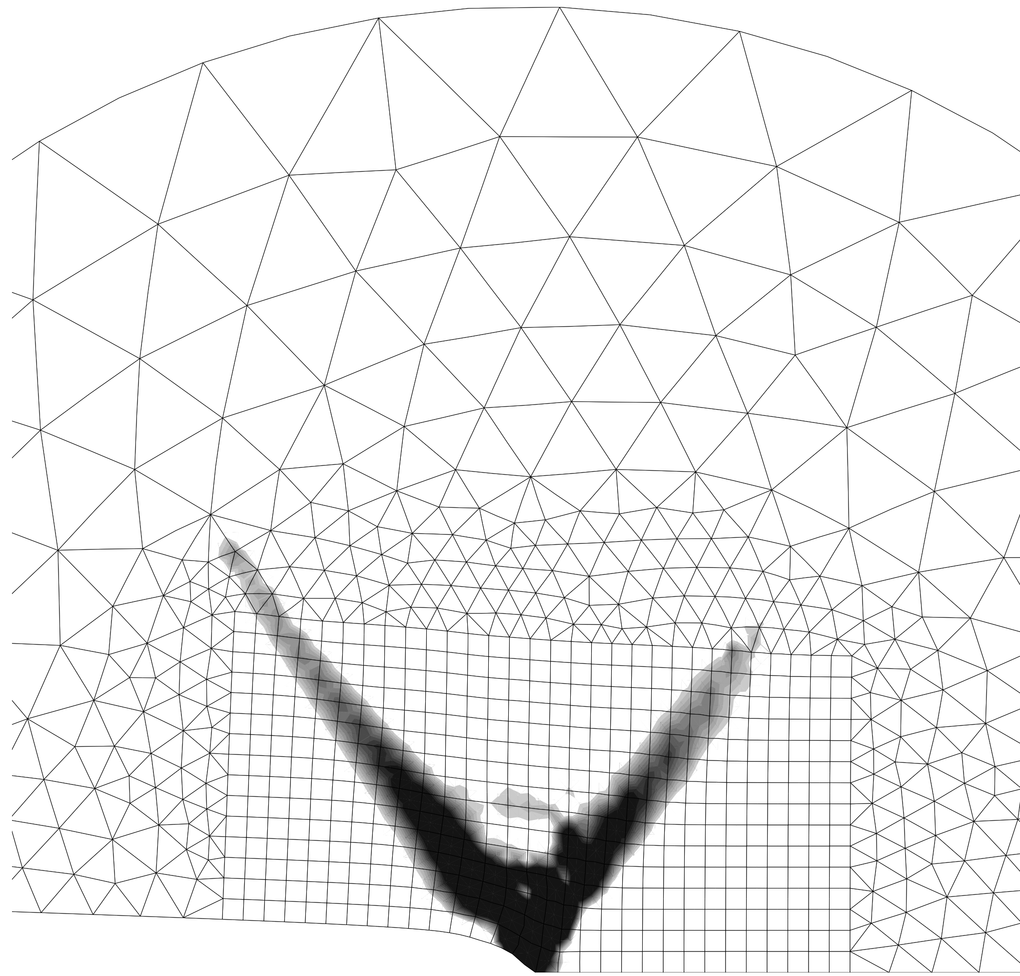

plastic slip (Cosserat)

Cosserat crystal plasticity at the crack tip

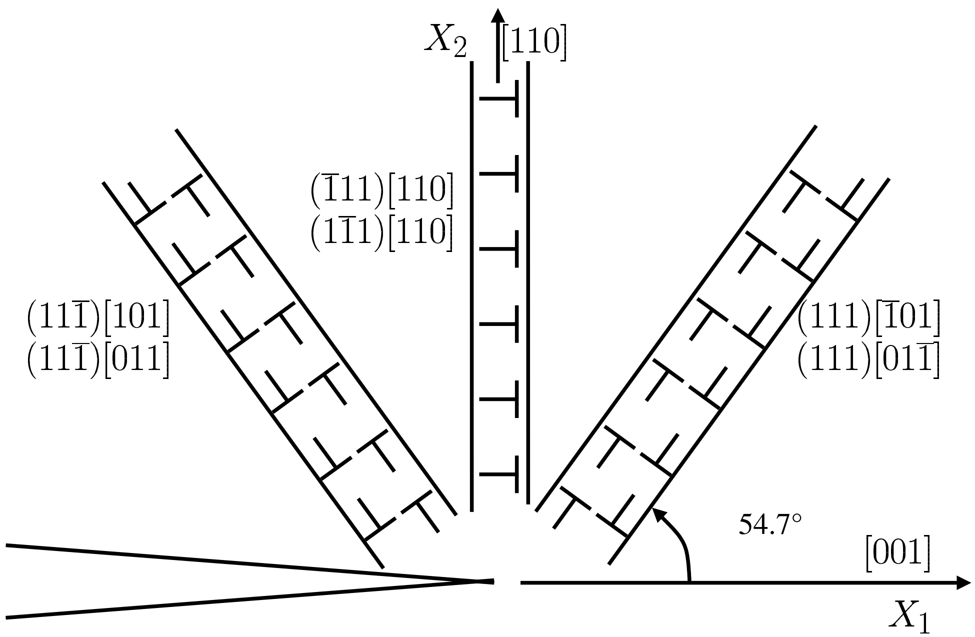

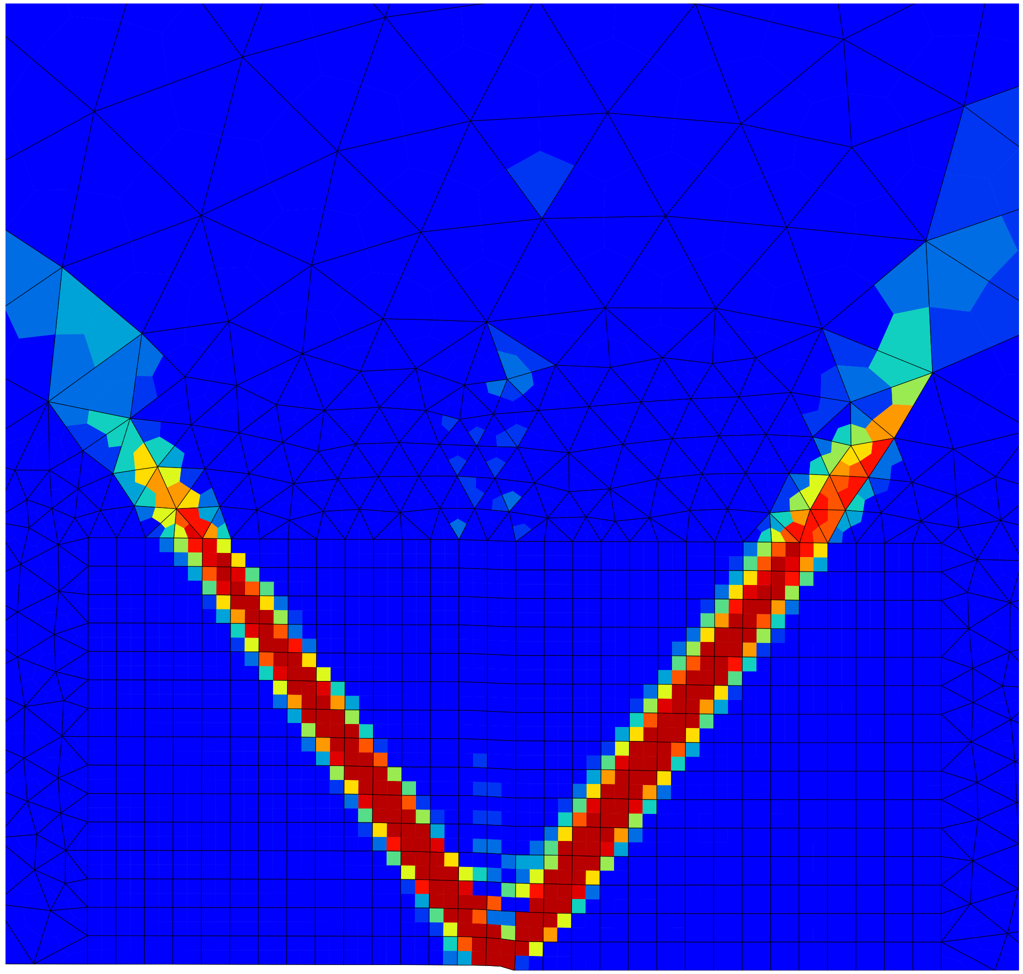

$(110)_{X_2}[001]_{X_1}$ crack orientation

lattice rotation (classical)

Cosserat crystal plasticity at the crack tip

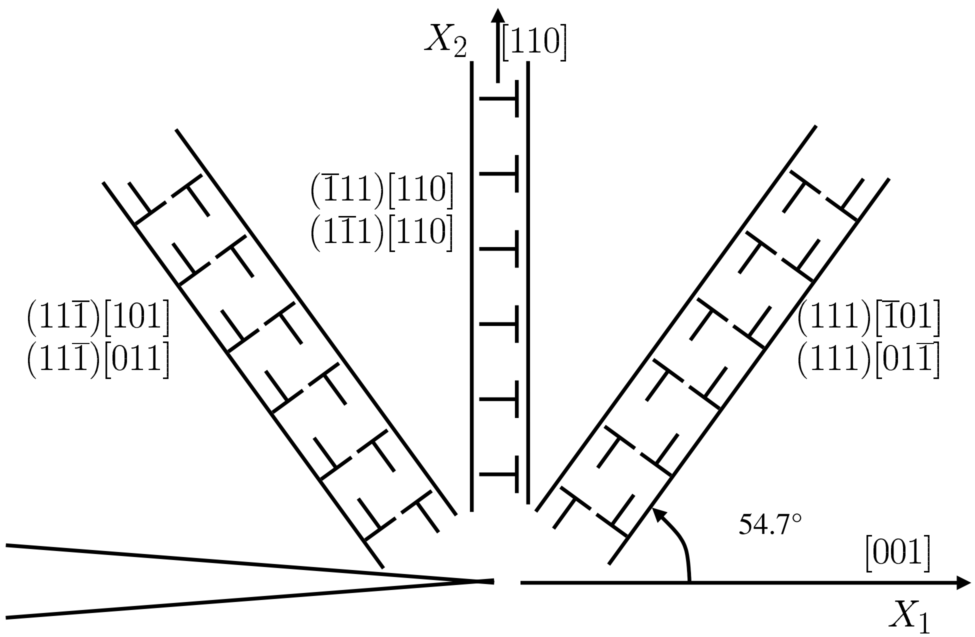

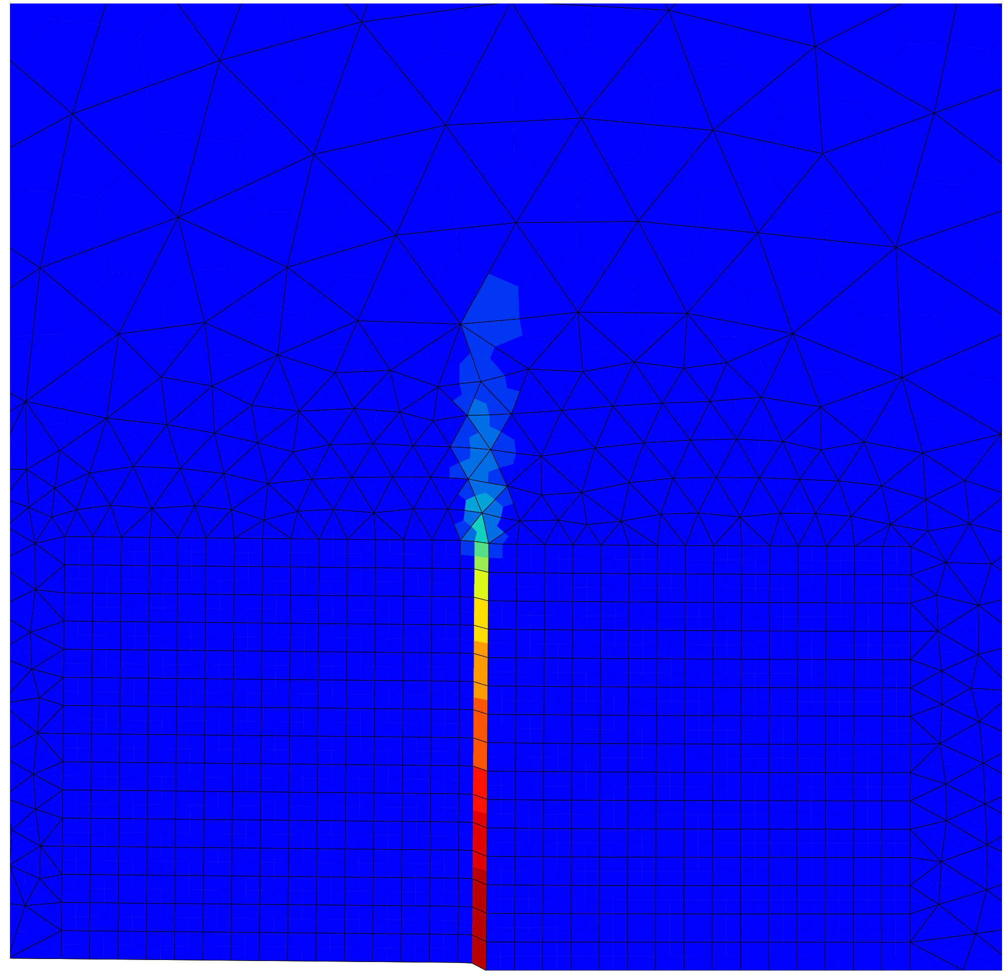

$(110)_{X_2}[001]_{X_1}$ crack orientation

plastic slip (Cosserat)

Control of the intensity of kink bands

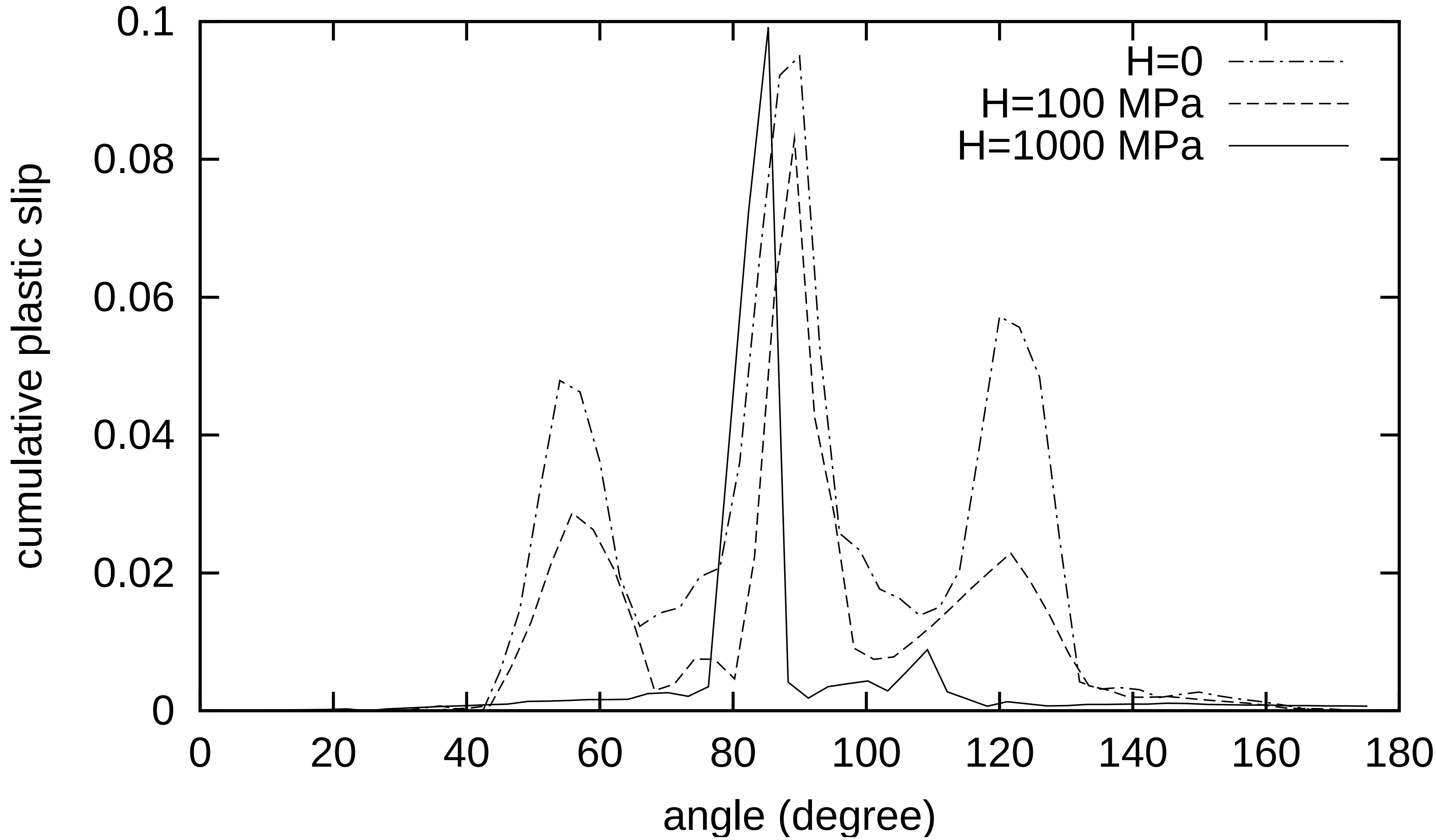

Cosserat crystal plasticity at the crack tip

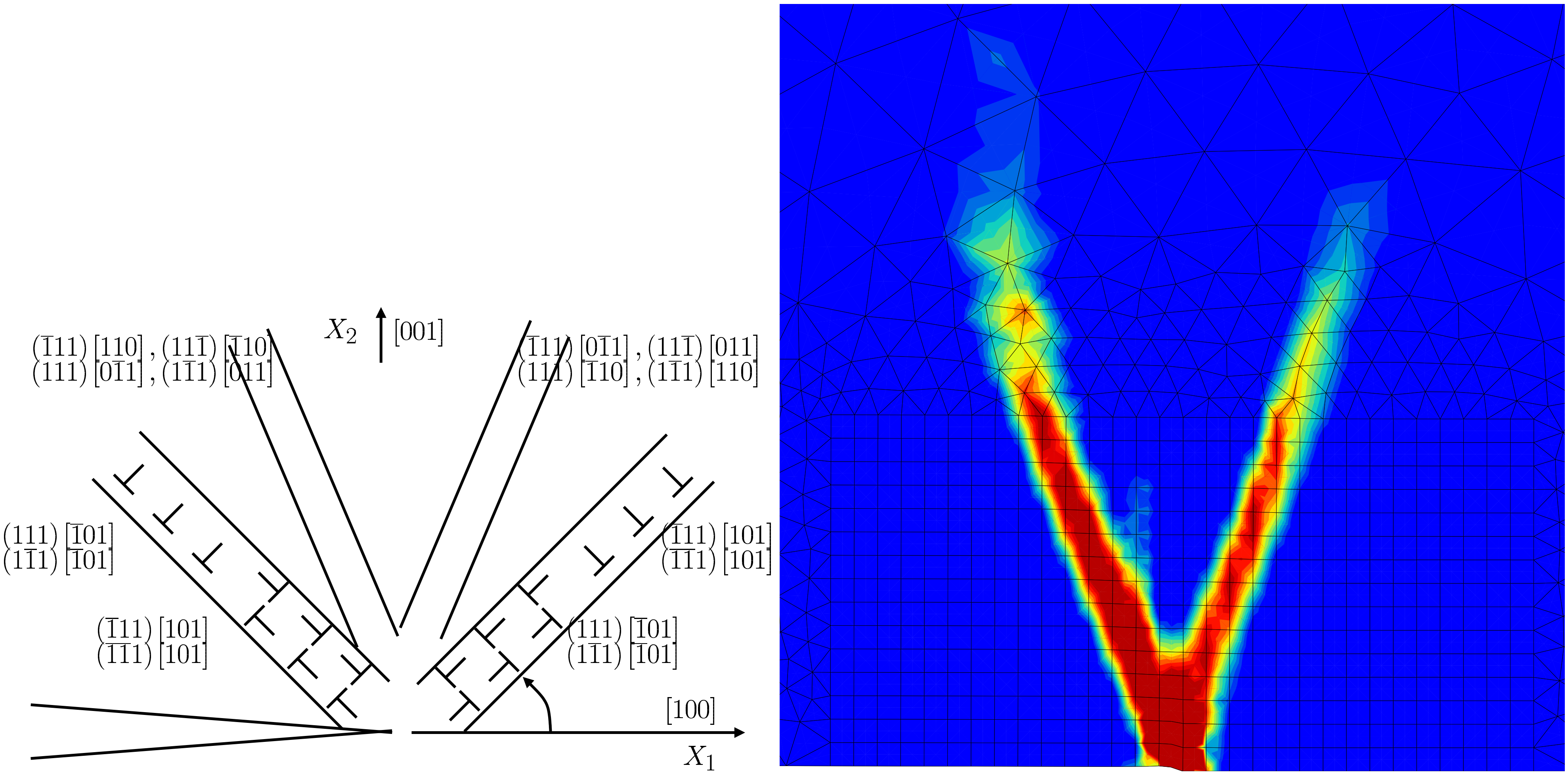

$(100)_{X_2}[001]_{X_1}$ crack orientation

Confrontations with experimentals results

Rice's solution was compared with several experimental results on metal single crystals

[Crompton, 1984] [Shield, 1996] [Crone, Shield, 2001] [Kysar, Briant, 2002]

crack $\Longleftrightarrow$ notch

plane strain $\Longleftrightarrow$ surface observation (3D effect)

perfect plasticity $\Longleftrightarrow$ strong hardening (copper...)

3D effects [Cuitiño, Ortiz, 1996] [Flouriot, 2003]

Single crystal nickel–base superalloys at room temperature are good candidates for such a comparison

3D effects ($(110)_{X_2}[001]_{X_1}$ crack orientation)

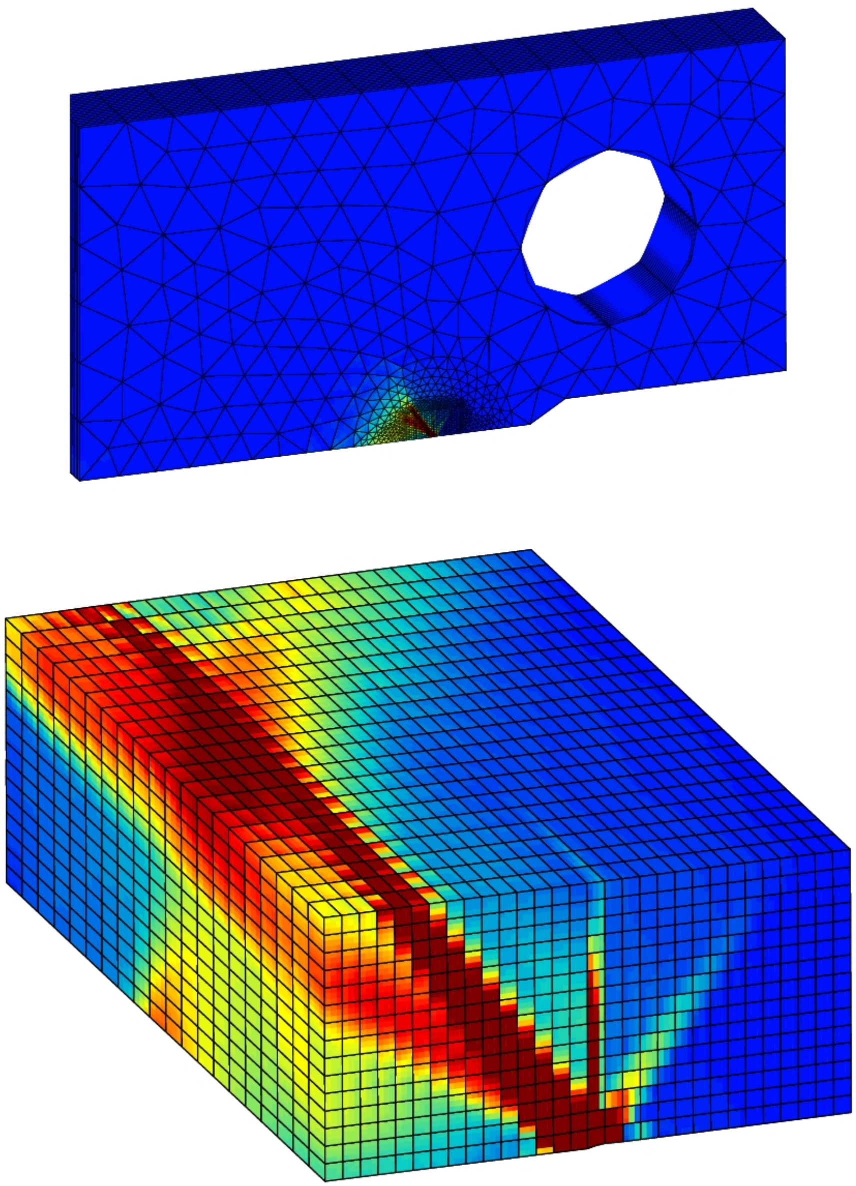

Mid section

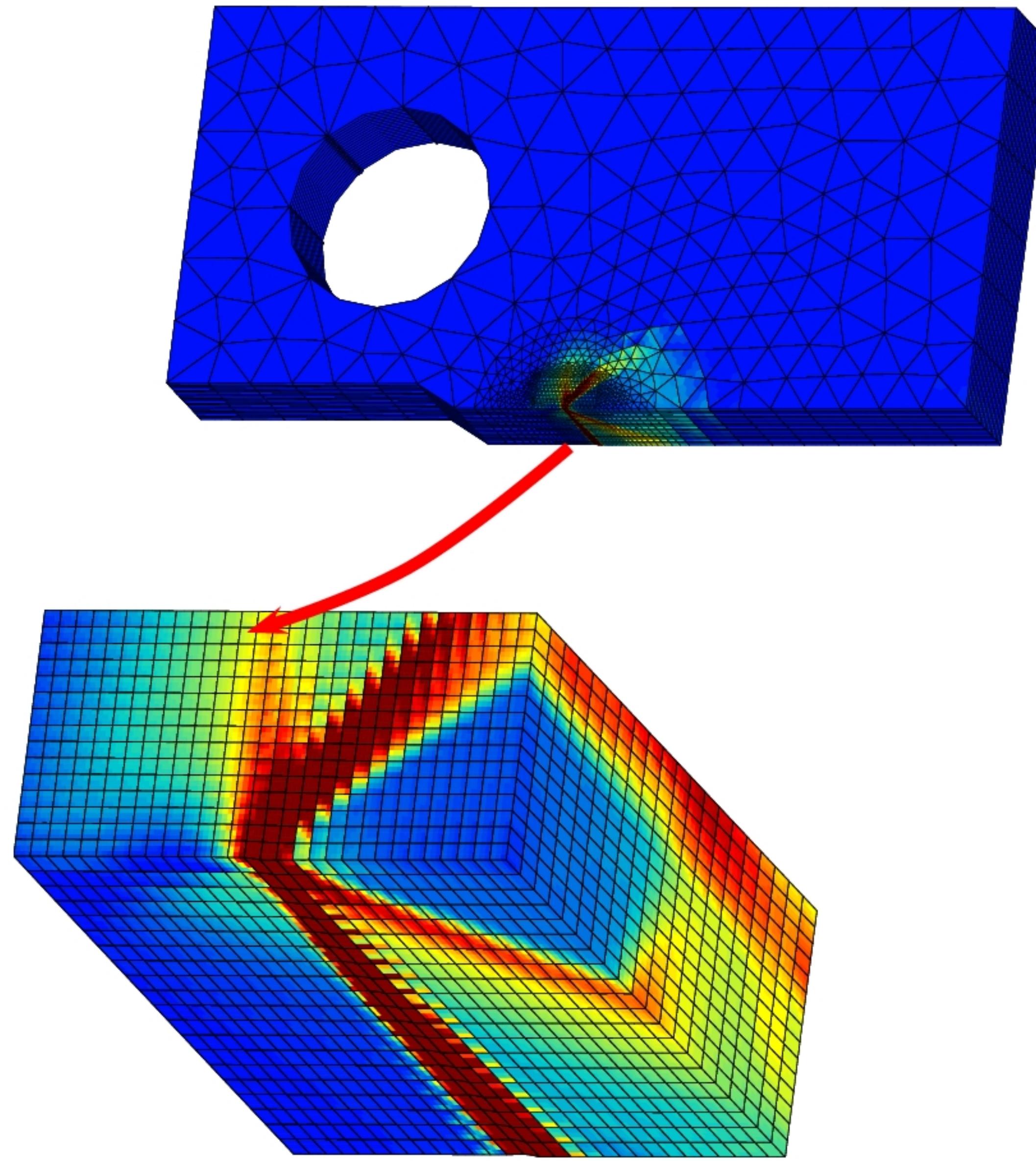

Surface

3D effects ($(110)_{X_2}[001]_{X_1}$ crack orientation)

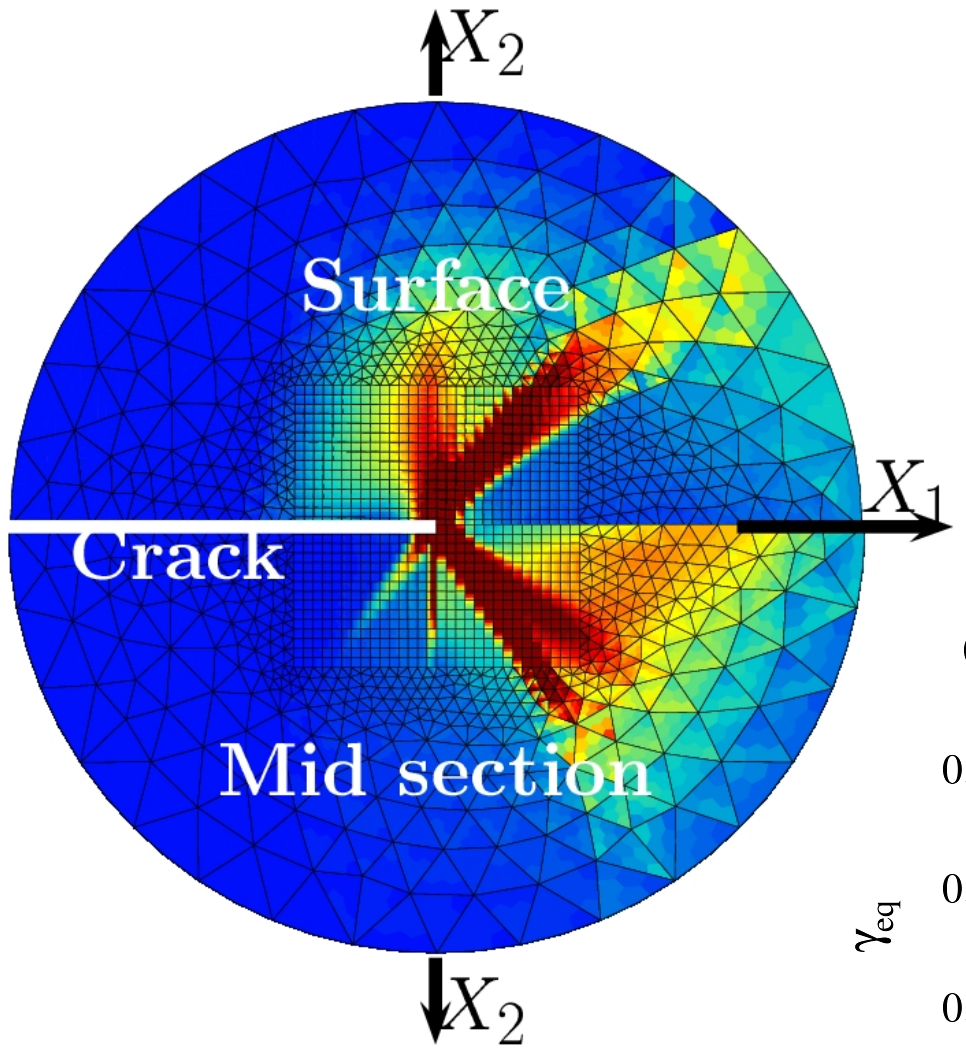

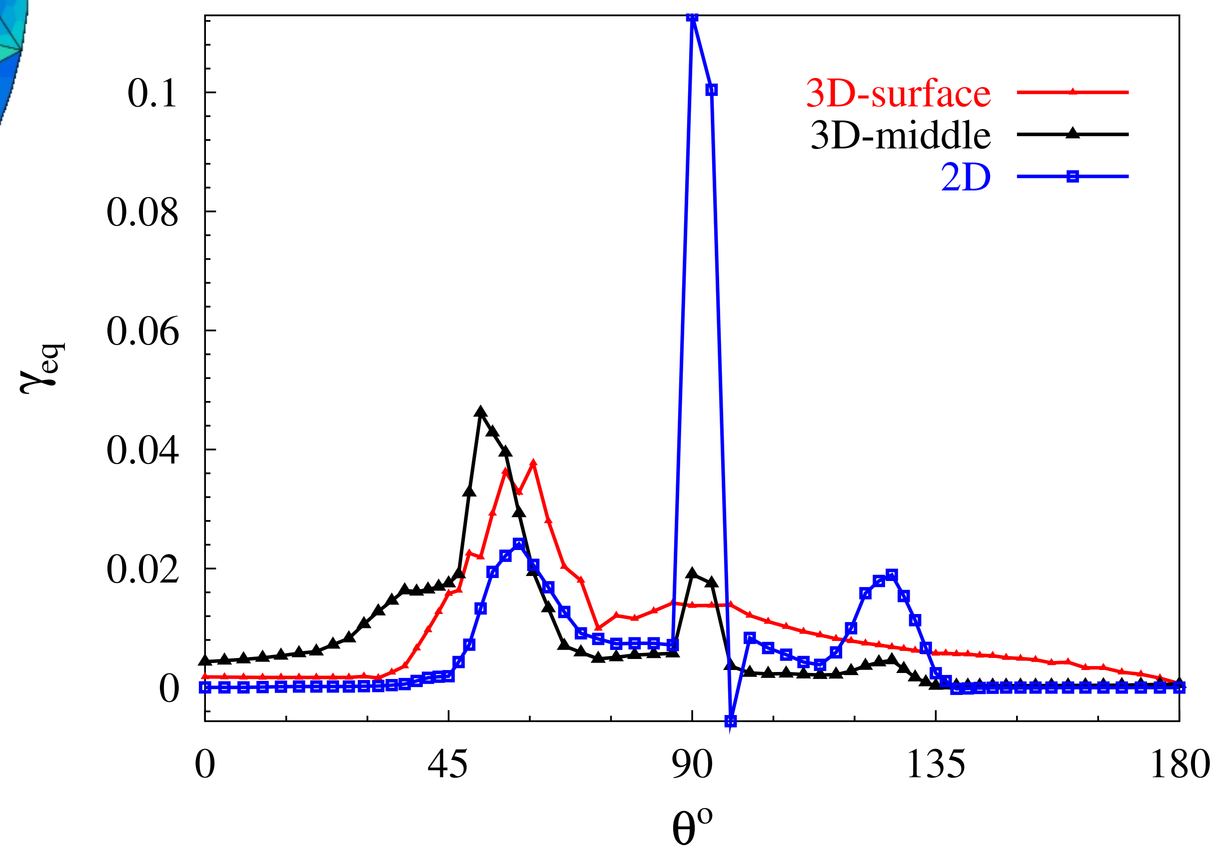

The experimental procedure

- Compact Tension Specimen CT16 , thickness=6mm
- Polishing
- Precrack at 650^oC
  - R=0.1
  - $\Delta K \searrow$
  - f=10Hz
- EBSD reference
- monotonous traction at 20^oC
- SEM observation
- interferometric and confocal observations
- EBSD on the surface and in the bulk of the specimen

Experimental results $(110)_{X_2}[001]_{X_1}$ *crack orientation*

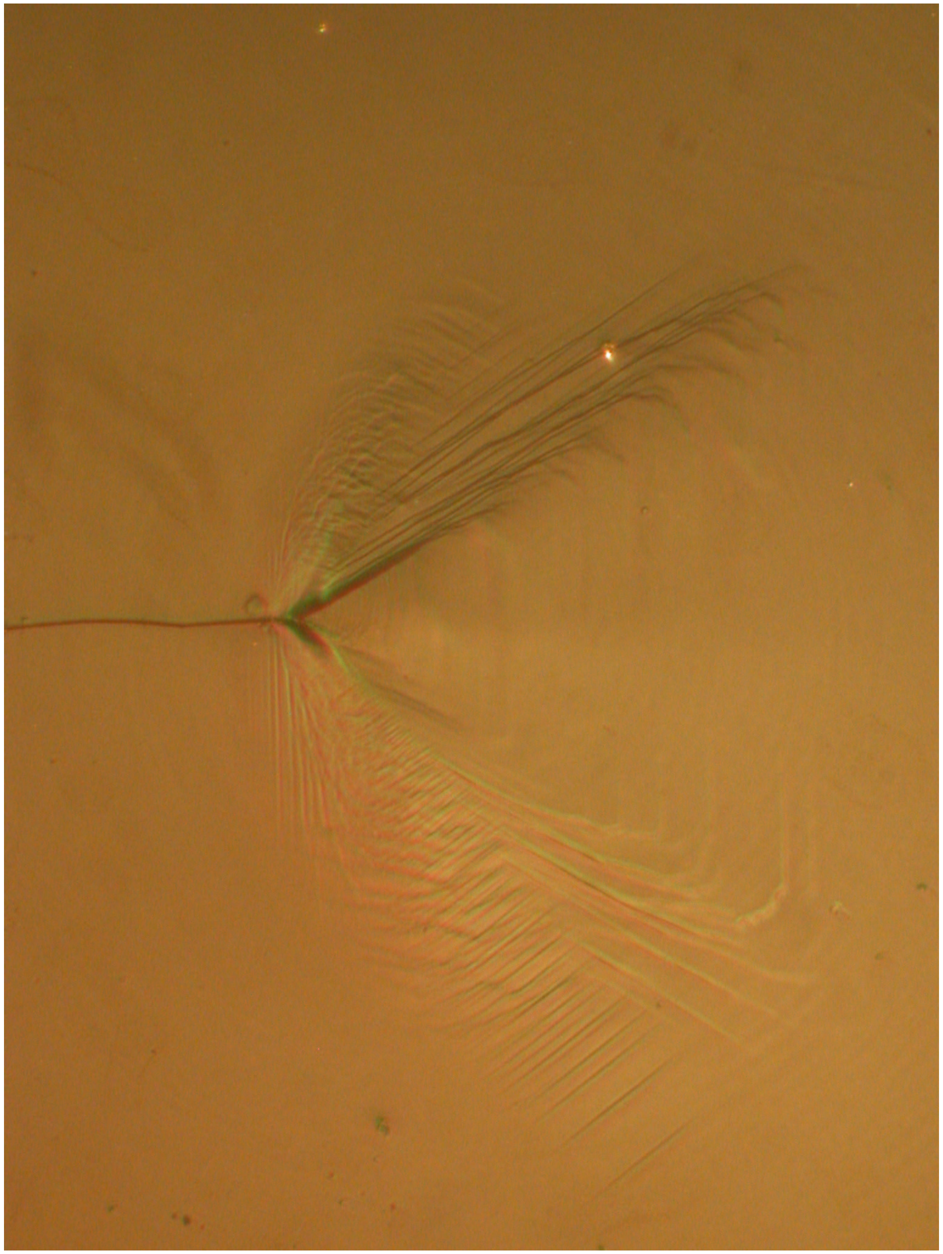

$K = 30 MPa\sqrt{m}$

Experimental results ($(110)_{X_2}[001]_{X_1}$ *crack orientation)*

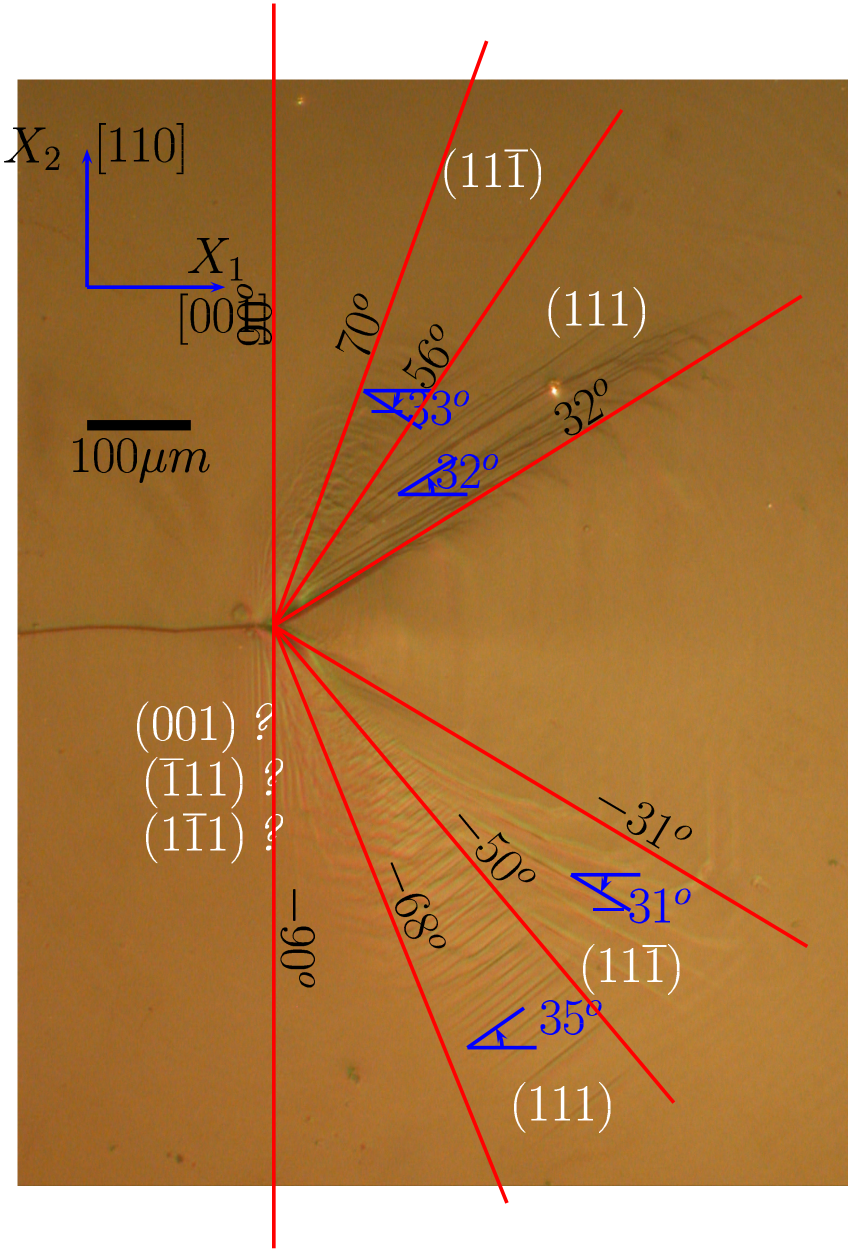

Comparison experiment/simulation

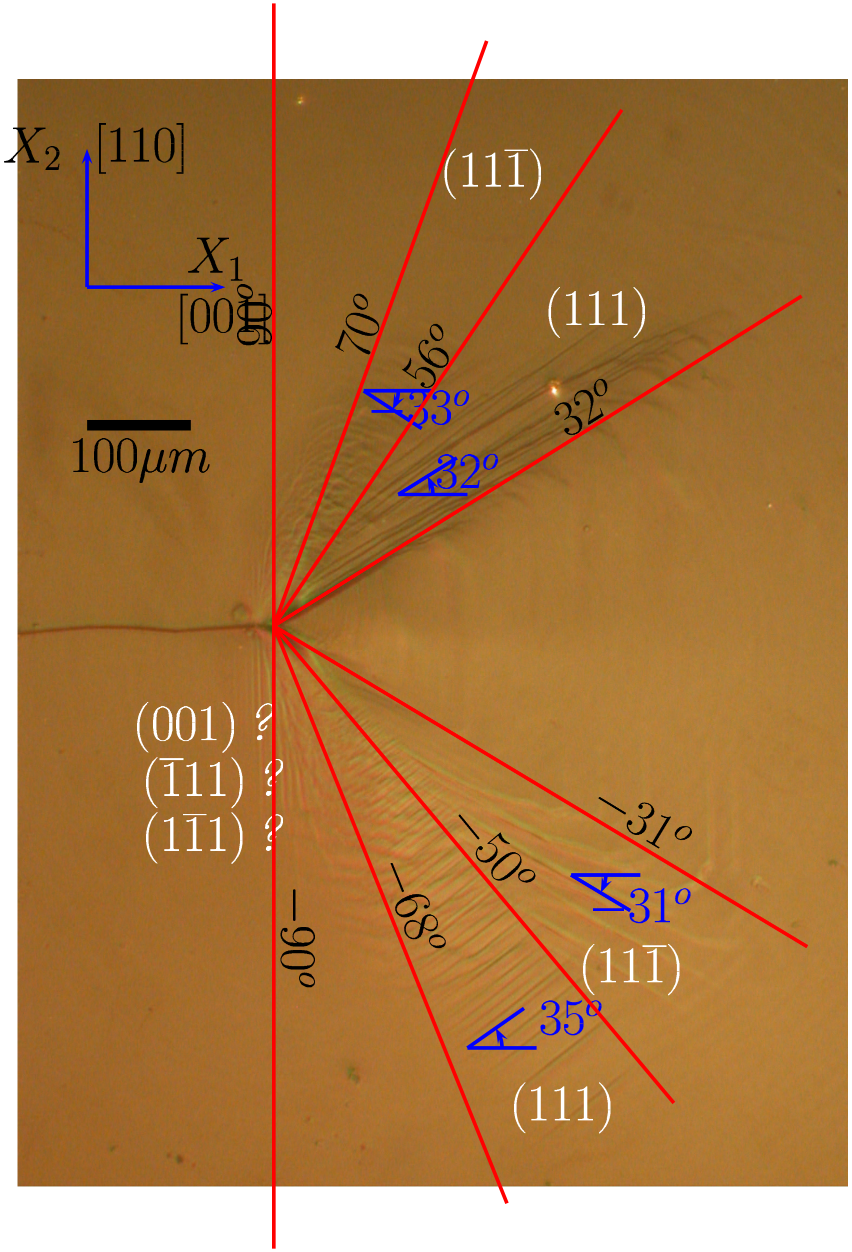

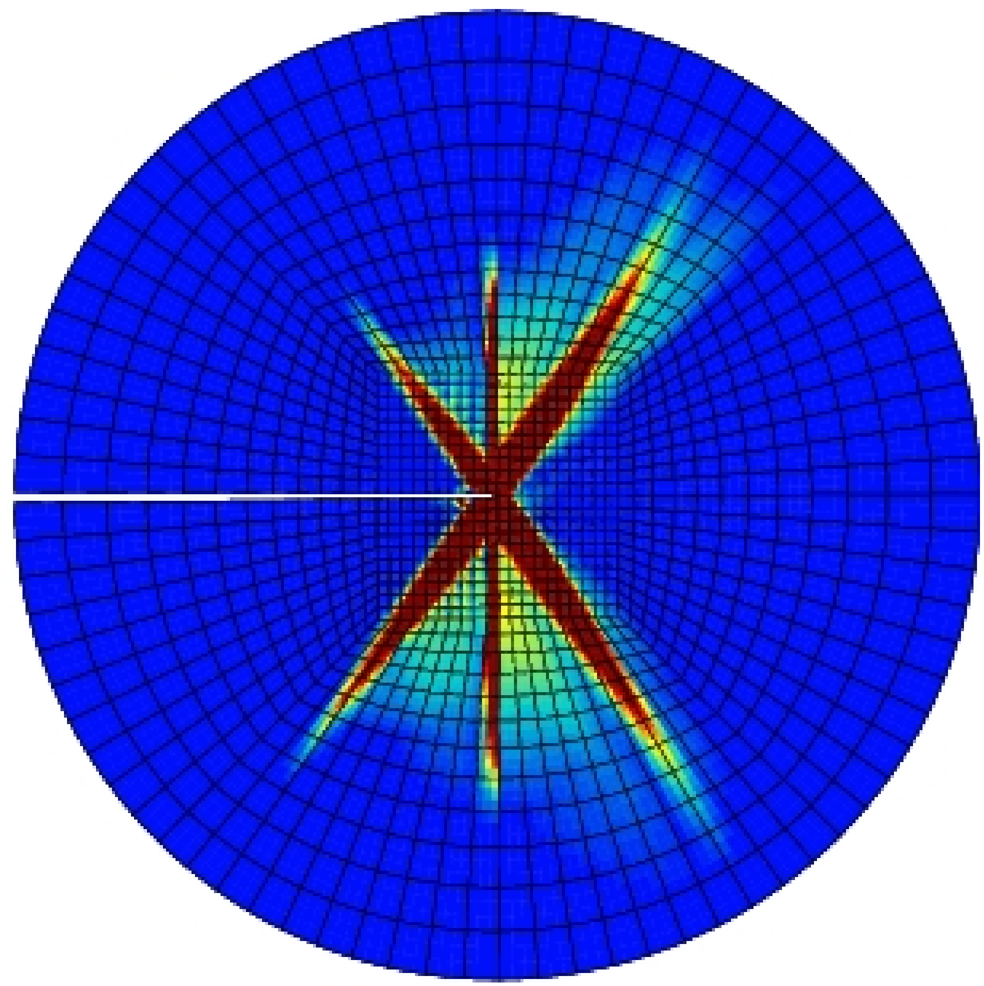

2D F.E. simulation

Comparison experiment/simulation ($(110)_{X_2}[001]_{X_1}$ crack orientation)

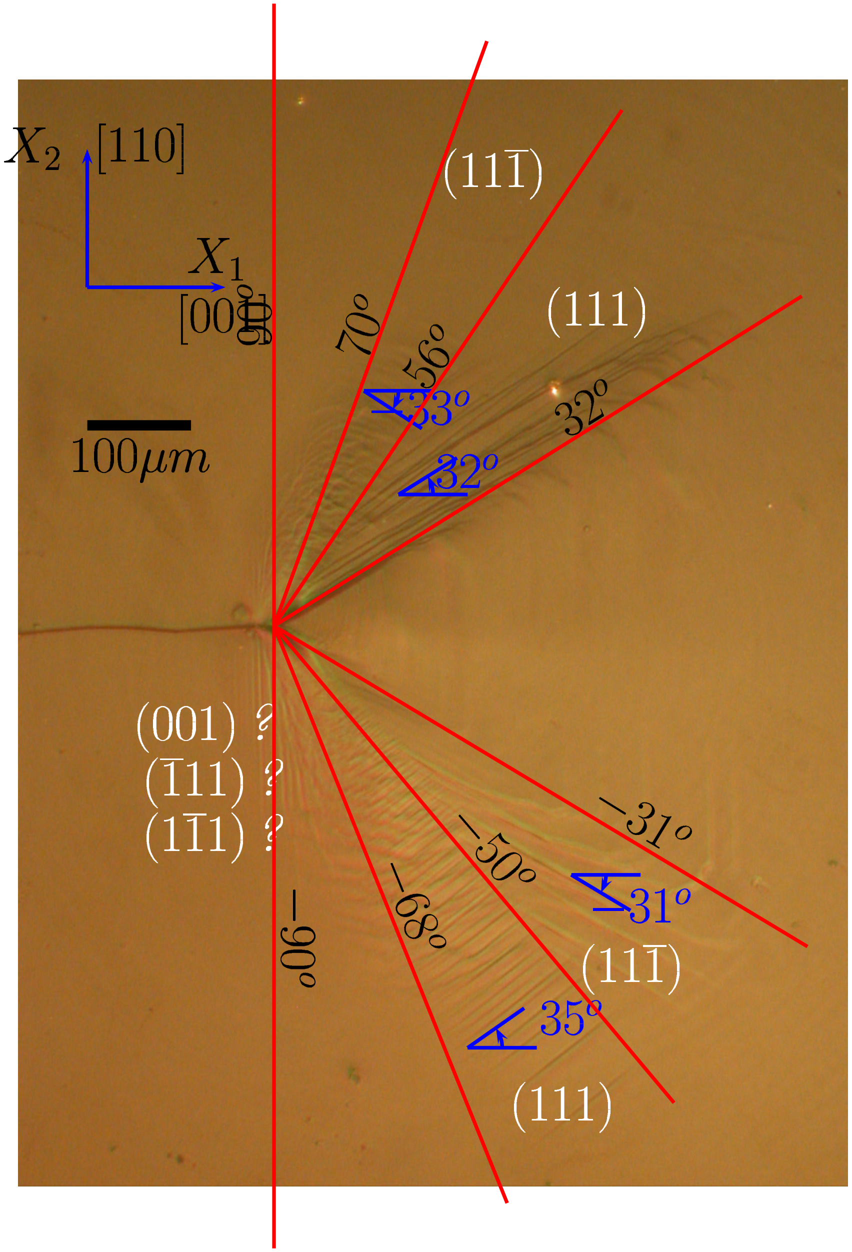

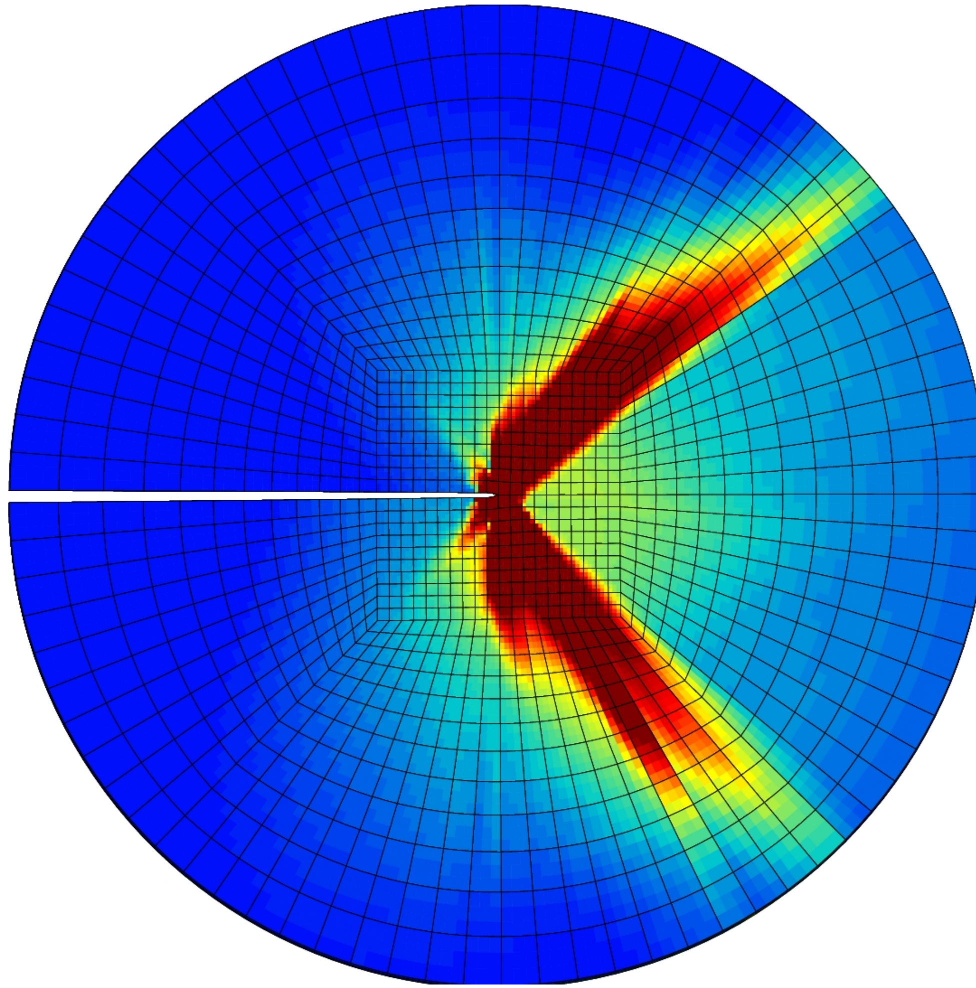

Surface of the specimen
3D F.E. Simulation

EBSD analysis ($(110)_{X_2}[001]_{X_1}$ crack orientation)

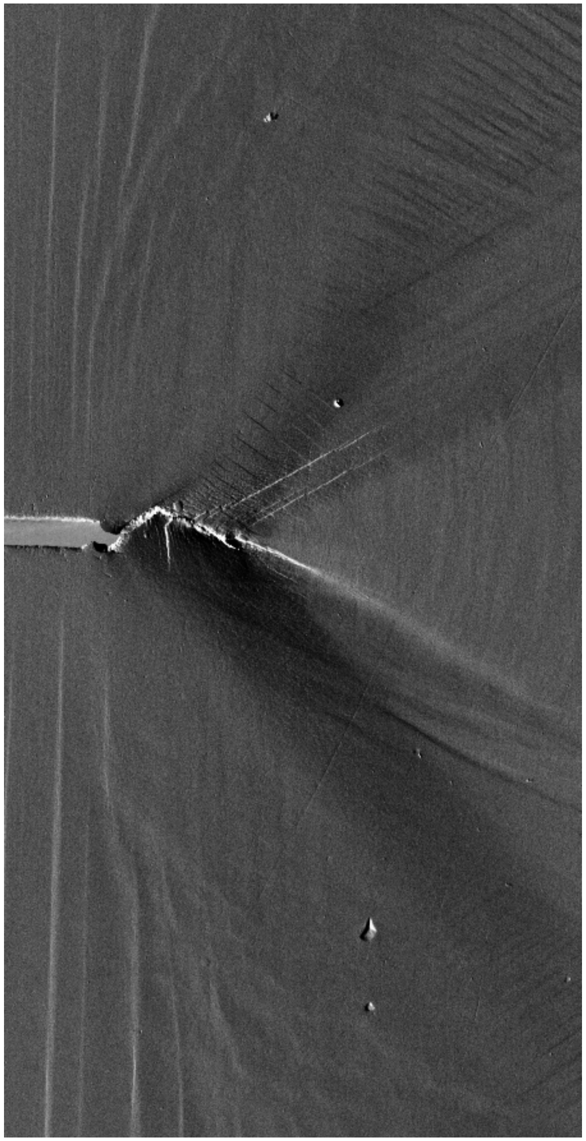

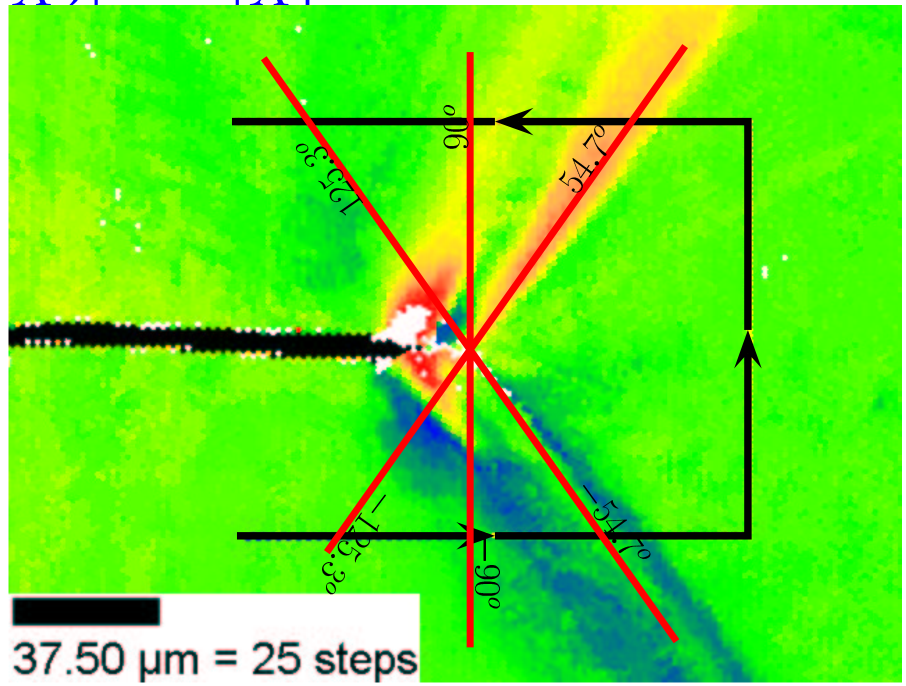

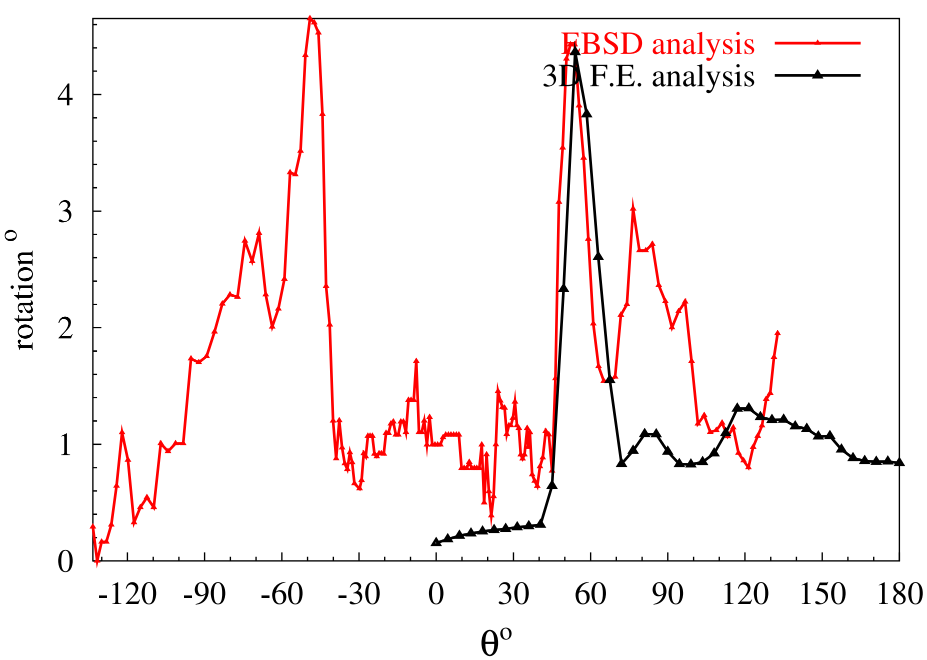

Fatigue crack growth

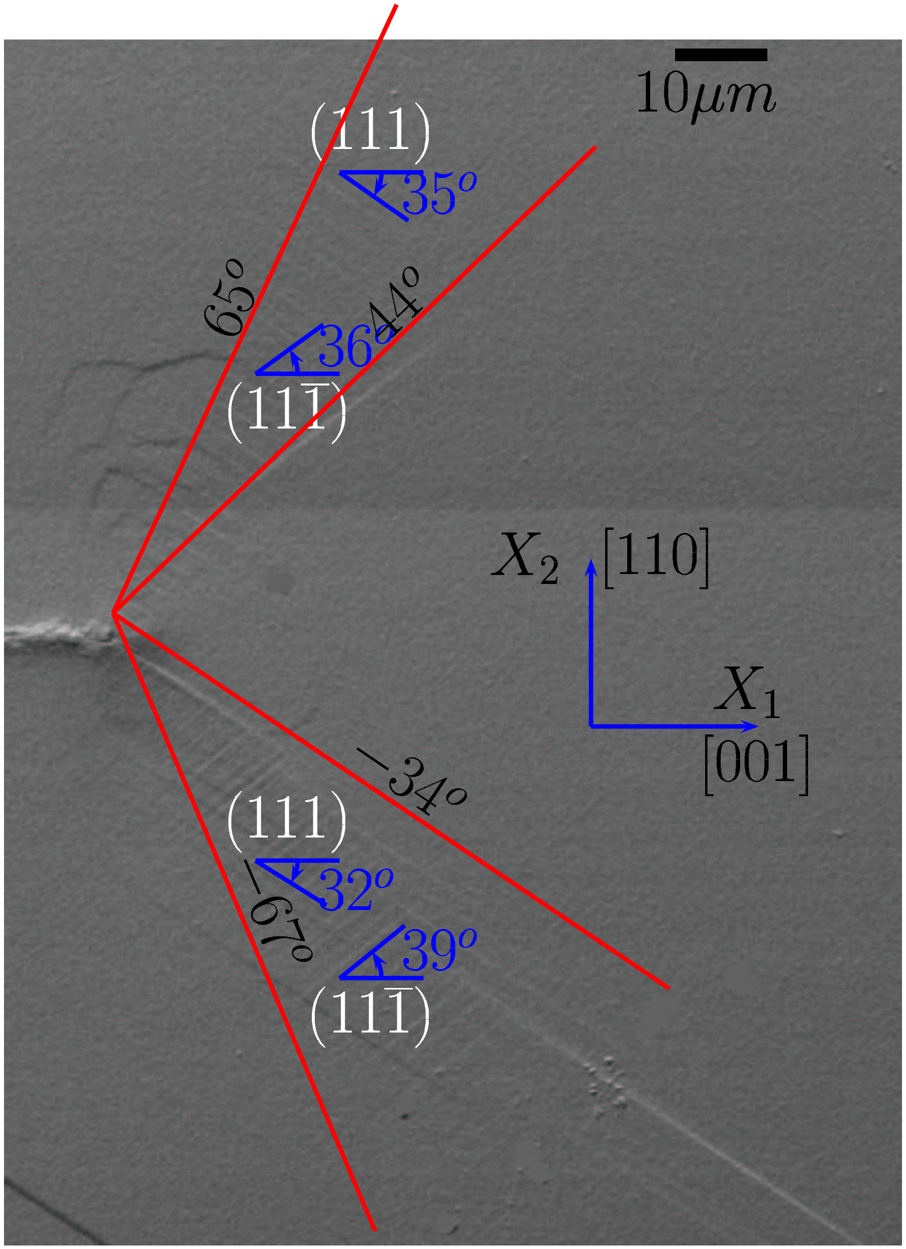

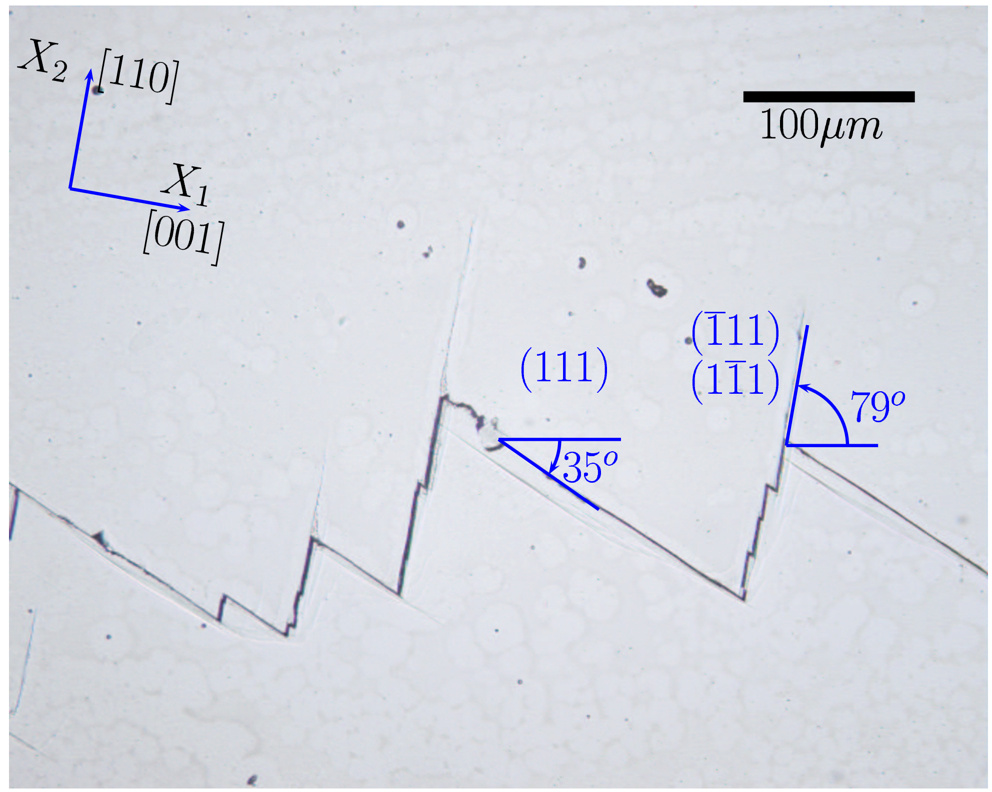

$(110)_{X_2}[001]_{X_1}$ crack orientation

Fatigue crack growth

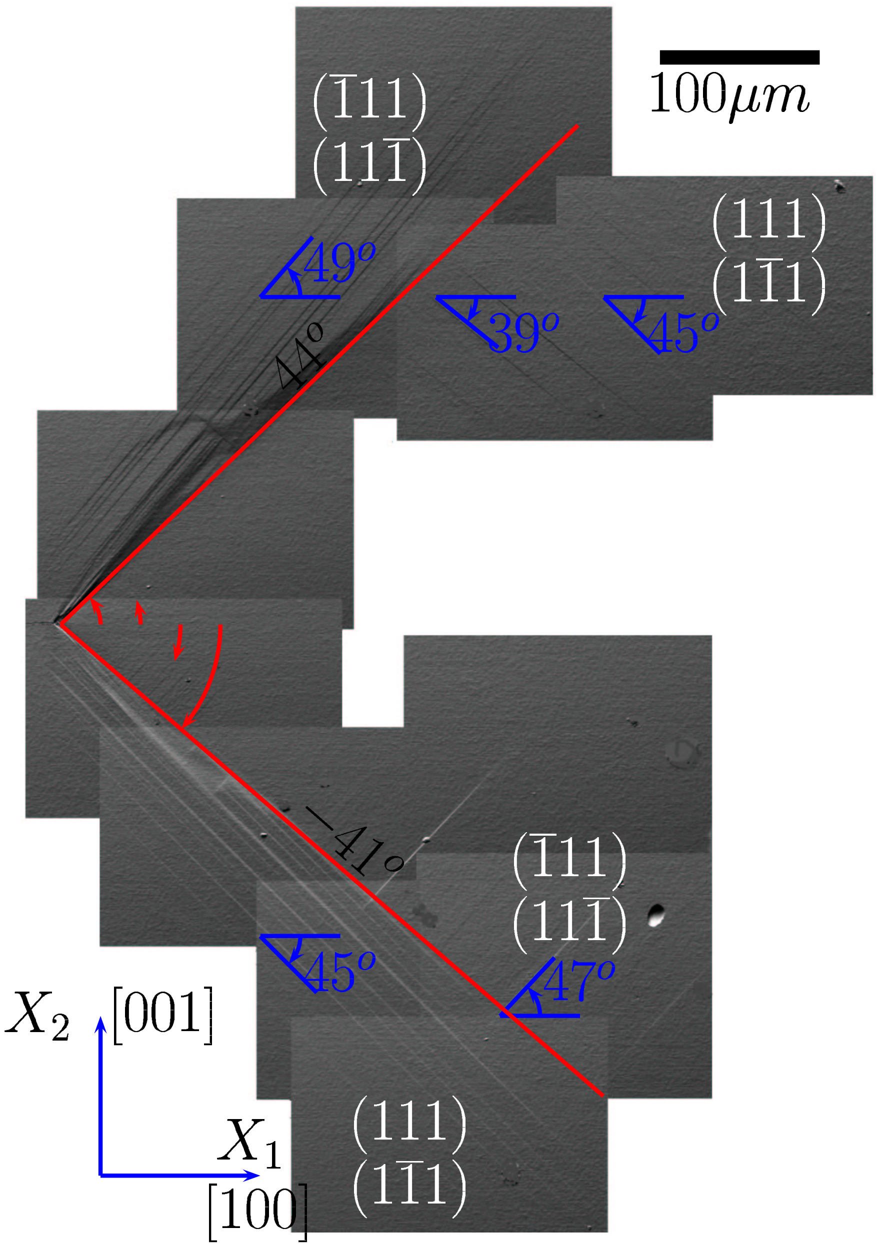

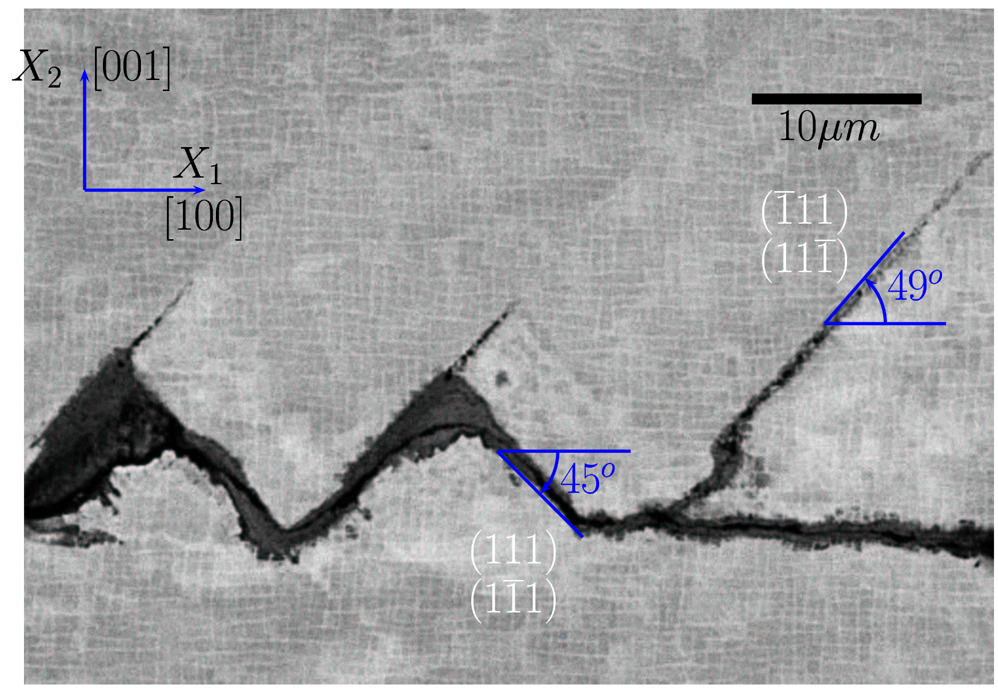

Conclusions

1. Kink bands exist at the crack tip in single crystal superalloys
2. Classical crystal plasticity provides a correct description of the crack tip field in single crystal superalloy CT specimens
3. Quantitative agreement is reached regarding the lattice rotation field around the crack tip
4. Generalized crystal plasticity makes it possible to control the intensity of kink bands
5. The type of localization bands plays a significant role in subsequent fatigue crack propagation

Notched Specimens